

An Adaptive and Stability-Promoting Layerwise Training Approach for Sparse Deep Neural Network Architecture

C G Krishnanunni* and Tan Bui-Thanh †

Abstract. This work presents a two-stage adaptive framework for progressively developing deep neural network (DNN) architectures that generalize well for a given training data set. In the first stage, a layerwise training approach is adopted where a new layer is added each time and trained independently by freezing parameters in the previous layers. We impose desirable structures on the DNN by employing manifold regularization, sparsity regularization, and physics-informed terms. We introduce a $\varepsilon - \delta$ -stability-promoting concept as a desirable property for a learning algorithm and show that employing manifold regularization yields a $\varepsilon - \delta$ stability-promoting algorithm. Further, we also derive the necessary conditions for the trainability of a newly added layer and investigate the training saturation problem. In the second stage of the algorithm (post-processing), a sequence of shallow networks is employed to extract information from the residual produced in the first stage, thereby improving the prediction accuracy. Numerical investigations on prototype regression and classification problems demonstrate that the proposed approach can outperform fully connected DNNs of the same size. Moreover, by equipping the physics-informed neural network (PINN) with the proposed adaptive architecture strategy to solve partial differential equations, we numerically show that adaptive PINNs not only are superior to standard PINNs but also produce interpretable hidden layers with provable stability. We also apply our architecture design strategy to solve inverse problems governed by elliptic partial differential equations.

Key words. Architecture adaptation, Manifold regularization, Physics-informed neural network, Sequential learning, Interpretable machine learning.

AMS subject classifications. 68T07, 68T05

1. Introduction. Deep neural networks (DNNs) have been prominent in learning representative hierarchical features from image, video, speech, and audio inputs [15, 23, 27, 38]. Some of the problems associated with training such deep networks include i) a possible large training set is necessary to overcome the over-fitting issue; ii) the architecture adaptability problem, e.g., any amendments to a pre-trained DNN require retraining even with transfer learning; and iii) GPU employment is almost mandatory due to massive network and data sizes. In particular, it is often unclear on the choice of depth and width of a network suitable for a specific problem. Existing neural architecture search algorithms rely on metaheuristic optimization, or combinatorial optimization, or reinforcement learning strategy to hopefully arrive at a reasonable architecture [61, 48, 50, 16, 43, 1, 37, 31]. However, these strategies involve training and evaluating many candidate architectures (possibly deep) in the process and are thus computationally expensive. Therefore, there is a need to develop a computationally tractable procedure for adaptively training/growing a DNN by leveraging information on the input data manifold and the underlying structure of the problems under consideration.

1.1. Related work. Layerwise training of neural networks is an approach that addresses the issue of the choice of depth of a neural network and the computational complexity involved

*Dept of Aerospace Engineering & Engineering Mechanics, UT Austin (krishnanunni@utexas.edu).

†Dept of Aerospace Engineering & Engineering Mechanics, UT Austin (tanbui@utexas.edu).

with training [56]. Many efforts have been proposed for growing neural architecture using this approach [22, 26, 9, 32, 55, 39, 44]. Hettinger et al. [22] showed that layers can be trained one at a time and the resulting DNN can generalize better. Belilovsky et al. [2] have further studied this approach for different convolutional neural networks. Kulkarni et al. [26] employed a kernel analysis of the trained layerwise deep networks. The weights for each layer are obtained by solving an optimization problem aiming at a better representation where a subsequent layer builds its representation on top of the features produced by a previous layer. Lengelle et al. [29] conducted a layer-by-layer training of multilayer perceptron by optimizing an objective function for internal representations while avoiding any computation of the network’s outputs. Bengio et al. [5] proposed a greedy layerwise unsupervised learning algorithm by initializing weights for each layer in a region near a good local minimum, giving rise to internal distributed representations that are high-level abstractions of the input, thereby bringing better generalization. Nguyen et al. [39] developed an analytic layerwise deep learning framework where an inverse layerwise training and a forward progressive learning approach are adopted.

Alternately, researchers have also considered growing the width gradually by adding neurons for a fixed depth neural network [53, 54]. Wynne-Jones [54] considered splitting the neurons (adding neurons) based on a principal component analysis on the oscillating weight vector. Liu et al. [53] developed a simple criterion for deciding the best subset of neurons to split and a splitting gradient for optimally updating the off-springs. Chen et al. [10] showed that replacing a model with an equivalent model that is wider (has more neurons in each hidden layer) allows the equivalent model to inherit the knowledge from the existing one and can be trained to further improve the performance.

It is noteworthy that while the works cited above show promising results for image classification tasks, layerwise training procedure can introduce a large number of parameters (especially in the context of a fully connected network) due to the addition of a new layer [22]. In such cases, it is important to recognize non-important parameters in an added layer and remove them. Further, layerwise training strategies in [2, 22, 51] do not ensure that the network output remains unchanged after a new layer is added thereby losing the performance achieved by previous layers. Moreover, recent work by Trinh et al. [51] observed overfitting in the early layers while performing a layerwise training strategy. Therefore, it is imperative to consider a layerwise training strategy that takes into account the following aspects: a) achieves light-weight hidden layers, i.e., automatically detects the non-important connections in an added layer and removes them; b) ensures that the network output remains unchanged after the addition of a new layer; c) mathematical principle to guide the design of each layer that prevents overfitting in early layers.

1.2. Our contributions. In this work, we use “*robustness*” as a desirable property for DNNs [24, 7, 58] and use this as a criterion to devise a strategy for progressively adapting DNN architecture for a given data-set. While recent work shows that over-parametrization could be necessary for “*robustness*” [7, 6], it is generally unclear how to distribute the parameters in a network (number of active connections in each hidden layer, number of layers). Our algorithm progressively builds a network by training one layer at a time while promoting *stability* for each layer and consequently promoting “*robustness*” as we will show. In particular, we set forth a sequential learning strategy where a learning task is divided into sub-tasks each of

which is learned before the next. Our idea is inspired by the mechanism of how the human brain learns [11]. A layerwise training strategy (Algorithm 2.1) where each layer is constrained to learn a specific task is adopted. To that end, when training each layer we incorporate a sparsity regularization for identifying the active/inactive parameters in each layer, a manifold regularization term [4] for promoting stability, and a physics-informed term [42] aiming to respect the underlying physics (if any). The key to our approach is to stimulate δ -stable neural hidden layers. Once layerwise training saturates, which we shall prove, we provide Algorithm 2.2 where a sequence of small networks is deployed to extract information from the residuals induced by the DNN generated from Algorithm 2.1. Using Algorithm 2.2 together with Algorithm 2.1 results in robustness and accuracy as we shall show. Since the procedure emphasizes training a small network/layer each time, it is computationally tractable for large-scale problems and is free from vanishing gradient problems. Numerical investigation on prototype regression problems, physics-informed neural networks (PINNs) for solving elliptic partial differential equations, and MNIST classification problems suggest that the proposed approach can outperform ad-hoc baseline networks.

2. Proposed methodology. The proposed architecture adaptation procedure has two stages: a) A layerwise training strategy for growing the depth of DNNs; and b) a sequential residual learning strategy in which a sequence of shallow networks is added for robust and accurate predictions. A brief outline of the two stages is provided below in subsection 2.1 and subsection 2.2.

2.1. Layerwise training strategy (Algorithm 2.1). One of the key aspects in our layerwise training strategy is to employ the Residual Neural Network (ResNet) [20, 21] which, as we will show, improves the training loss accuracy when adding new layers. In this work, all the matrices and vectors are represented in boldface. Notation $(\cdot)^{(i)}$ denotes the quantities (matrix, vector, scalar, set, or function) for the i^{th} layer. Consider a regression/classification problem of O outputs and S input training features. Given inputs $\mathbf{x}_i \in \mathbb{R}^S$ for $i \in \{1, 2, \dots, M\}$ organized column-wise into a matrix $\mathbf{X} \in \mathbb{R}^{S \times M}$, we denote the corresponding network outputs as $\mathbf{y}_i \in \mathbb{R}^O$ which can also be organized column-wise into a matrix $\mathbf{Y} \in \mathbb{R}^{O \times M}$. The corresponding true labels are denoted as $\mathbf{c}_i \in \mathbb{R}^O$ and in stacked column-wise as $\mathbf{C} \in \mathbb{R}^{O \times M}$. We denote $\mathbf{Y}^{(1)} = h^{(1)}(\mathbf{W}^{(1)}\mathbf{X} + \mathbf{b}^{(1)})$ as the output of the first (optional) upsampling/downsampling layer, where $\mathbf{W}^{(1)}$ and $\mathbf{b}^{(1)}$ represents the weight matrix and bias vector for this layer. $\mathbf{Y}^{(1)}$ is then propagated forward through a L layers of ResNet as:

$$\begin{aligned}
 \mathbf{Y}^{(1)} &= h^{(1)}\left(\mathbf{W}^{(1)}\mathbf{X} + \mathbf{b}^{(1)}\right), \\
 (2.1) \quad \mathbf{Y}^{(i+1)} &= \mathcal{R}^{(i)}\left(\mathbf{Y}^{(i)}\right) + h^{(i+1)}\left(\mathbf{W}^{(i+1)}\mathcal{R}^{(i)}\left(\mathbf{Y}^{(i)}\right) + \mathbf{b}^{(i+1)}\right), \text{ for } i = 1, \dots, L-1, \\
 \mathbf{Y}^{(L+1)} &= h_{pred}\left(\mathbf{W}_{pred}\mathcal{R}^{(L)}\left(\mathbf{Y}^{(L)}\right) + \mathbf{b}_{pred}\right),
 \end{aligned}$$

where $h^{(i+1)}$, $\mathbf{W}^{(i+1)}$, $\mathbf{b}^{(i+1)}$ are the activation function, weight matrix, and bias vector of the $(l+1)$ th layer, while h_{pred} , \mathbf{W}_{pred} , \mathbf{b}_{pred} are the activation function, weight matrix, and bias vector of the output layer, and $\mathcal{R}^{(i)}$ represents an optional linear transformation for feature scaling on each hidden layer (we only need this for theoretical purpose in Proposition 3.9).

In order to impose desirable properties for the layerwise training strategy, we incorporate there different regularization terms, namely, (a) Manifold regularization, (b) Physics-informed regularization, and (c) Sparsity regularization.

1. *Manifold Regularization (Data-dependent regularization)*: Manifold regularization exploits the geometry of marginal distribution where we assume that the input data is not drawn uniformly from input space \mathbb{R}^S but lies on a submanifold $\mathcal{M} \subset \mathbb{R}^S$ [4, 17]. Let μ be a probability measure with support on \mathcal{M} . Let $\nabla_{\mathcal{M}} f(x)$ denote the gradient of f along the manifold \mathcal{M} (see, e.g., Do Carmo [14] for an introduction to differential geometry and definition of gradient along the manifold). To force the gradient of the learned function (each hidden layer in our case) to be small whenever the probability of drawing a sample is large, one can define the following H^1 -like regularization term [4, 24, 45, 28]:

$$(2.2) \quad \Phi_m = \int_{\mathcal{M}} \left\| \nabla_{\mathcal{M}} \mathbf{y}_{\boldsymbol{\theta}}^{(l)}(\mathbf{x}) \right\|_2^2 d\mu(\mathbf{x}) \approx \frac{1}{M^2} \sum_{i,j} \beta_{ij} \left\| \mathbf{y}_{\boldsymbol{\theta}}^{(l)}(\mathbf{x}_i) - \mathbf{y}_{\boldsymbol{\theta}}^{(l)}(\mathbf{x}_j) \right\|_2^2,$$

where $\mathbf{y}_{\boldsymbol{\theta}}^{(l)}(\mathbf{x})$ is the output of the l^{th} hidden layer for an input \mathbf{x} , $\boldsymbol{\theta}$ represents the trainable network parameters up to layer l , and the indices i and j on the right hand side of (2.2) varies from 1 to M to represent the pairwise comparison between all training samples. Note that the convergence of the right-hand side to the left-hand side of (2.2) is valid under certain conditions and when choosing exponential weights for the similarity matrix β_{ij} [4, 3]. However, (2.2) is expensive to compute when M is large due to the computational complexity of $\mathcal{O}(M^2)$. In order to reduce the computational complexity, the similarity matrix β_{ij} in (2.2) is computed based on the pairwise must-link constraint set [34]:

$$(2.3) \quad \beta_{ij} = \begin{cases} \beta_p & \text{for } \mathbf{c}_i^{(p)} = \mathbf{c}_j^{(p)}, \\ 0 & \text{otherwise,} \end{cases}$$

where $\mathbf{c}_i^{(p)}$ denotes the label assigned to training input \mathbf{x}_i belonging to cluster/class C_p for a classification task, and $\beta_p \geq 0$ and bounded such that $\beta_p \neq 0$ for at least one p . For regression problems, one may use clustering algorithms such as K-means clustering for computing β_{ij} in (2.3), where data points in the same clusters are assigned the same labels, and different clusters have different labels. Inspired by this choice of similarity matrix β_{ij} in practice, we consider a new form of manifold regularization Φ_m as follows:

$$(2.4) \quad \begin{aligned} \Phi_m &= \sum_{p=1}^K \beta_p \int_{\mathcal{M}_p} \int_{\mathcal{M}_p} \left\| \mathbf{y}_{\boldsymbol{\theta}}^{(l)}(\mathbf{x}) - \mathbf{y}_{\boldsymbol{\theta}}^{(l)}(\mathbf{y}) \right\|_2^2 d\mu_p(\mathbf{x}) d\mu_p(\mathbf{y}) \\ &\approx \sum_{p=1}^K \left[\frac{\beta_p}{m_p^2} \sum_{\mathbf{x}_i, \mathbf{x}_j \in C_p} \left\| \mathbf{y}_{\boldsymbol{\theta}}^{(l)}(\mathbf{x}_i) - \mathbf{y}_{\boldsymbol{\theta}}^{(l)}(\mathbf{x}_j) \right\|_2^2 \right], \end{aligned}$$

where μ_p is the probability measure with support \mathcal{M}_p and $\cup_p \mathcal{M}_p = \mathcal{M}$, K denotes the total number of clusters, and m_p denotes the number of samples in C_p . In [Propo-](#)

sition 3.9, we will show that penalizing (2.4) helps in promoting stability for hidden layers during the learning process.

2. *Physics-informed regularization:* In addition to the training data, if one is also provided with information on the underlying physics of the problem, then each hidden layer in our proposed approach can be interpretable (see section 4.2). For example, given a forward operator \mathcal{G} of algebraic/ differential equation type:

$$(2.7) \quad \mathcal{G}(\hat{\mathbf{x}}, \hat{\mathbf{y}}) = \mathbf{0}, \quad \hat{\mathbf{x}} \in \mathbb{R}^{\mathbf{S}}, \quad \hat{\mathbf{y}} \in \mathbb{R}^{\mathbf{O}},$$

a physics-informed regularization term can be defined as

$$(2.8) \quad \Phi_p = f[\mathcal{G}(\hat{\mathbf{x}}_1, \mathcal{N}(\hat{\mathbf{x}}_1, \boldsymbol{\theta})), \mathcal{G}(\hat{\mathbf{x}}_2, \mathcal{N}(\hat{\mathbf{x}}_2, \boldsymbol{\theta})), \dots, \mathcal{G}(\hat{\mathbf{x}}_r, \mathcal{N}(\hat{\mathbf{x}}_r, \boldsymbol{\theta}))] \in \mathbb{R},$$

where \mathcal{N} represents the output of the ResNet in (2.1) with parameters $\boldsymbol{\theta}$, $\{\hat{\mathbf{x}}_1 \dots \hat{\mathbf{x}}_r\}$ is the set of collocation points, and f is a user-defined loss.

3. In addition, we also employ the L_1 regularization (sparsity promoting regularization) denoted as $\Phi_s(\boldsymbol{\theta})$ to promote learning only the important weights/biases in a layer.

Putting all the regularizations together, our layerwise training process is shown in [Algorithm 2.1](#). [Algorithm 2.1](#) starts with training (minimizing the loss function (2.5)) a two-hidden layer network where the first layer is the (optional) upsampling/downsampling layer. Once, this network is trained, a new layer is added with the weights and biases initialized as zero (line 6 in [Algorithm 2.1](#)). Keeping parameters in the previous layers fixed, the newly added layer is trained (minimizing the cost function (2.6)). The procedure is repeated until a termination criteria is satisfied (line 4 in [Algorithm 2.1](#)). Other details are provided in [Algorithm 2.1](#).

2.2. Sequential residual learning strategy ([Algorithm 2.2](#)). As we shall show (see [Corollary 3.16](#)), even though [Algorithm 2.1](#) proposed in this work prevents overfitting in early layers, training saturates after a certain critical layer. To overcome this issue, we add a post-processing stage for [Algorithm 2.1](#) in order to further decrease the training loss without overfitting the data. This stage is named the “sequential residual learning strategy” where one trains a sequence of neural networks to extract information from the residual resulting from [Algorithm 2.1](#). The procedure is shown in [Algorithm 2.2](#). [Algorithm 2.2](#) starts by generating new training labels (residuals) using a pre-trained network \mathcal{N} as demonstrated in line 4 of [Algorithm 2.2](#). A shallow network \mathcal{Q}_2 is then trained for a limited number of epochs as shown in line 6 of [Algorithm 2.2](#). Note that this is essential for preventing overfitting on the residuals and promoting δ -stability as will be discussed later in [subsection 3.2](#). The procedure is then repeated until a termination criteria is satisfied (line 2 in [Algorithm 2.2](#)).

3. An analysis of [Algorithm 2.1](#) and [Algorithm 2.2](#). In this section, we introduce key concepts— δ -stability and approximate δ -robustness—that drive the development of our approach. In particular, we prove how the design of [Algorithm 2.1](#) promotes δ -stability for each hidden layer ([subsection 3.1.1](#)) while also analyzing training saturation problems that might arise from certain hyperparameter settings ([subsection 3.1.2](#)). Lastly, [subsection 3.2.1](#) analyzes the role of [Algorithm 2.2](#) in promoting robustness.

3.1. Layerwise training [Algorithm 2.1](#). In [Algorithm 2.1](#), the input features are transformed through layers with previously trained weights and biases to create a new learning

Algorithm 2.1 Layerwise training Algorithm

Input: Training data \mathbf{X} , labels \mathbf{C} , validation data \mathbf{X}_1 , validation labels \mathbf{C}_1 , loss function Φ_d , loss tolerance ε_η for addition of layers, node tolerance ρ for thresholding of nodes, initial regularization parameters (α, τ, γ) , similarity matrix β_{ij} , the number of neurons in each hidden layer N_o .

Initialize: $\mathbf{U}, \mathbf{b}^{(1)}, \mathbf{W}^{(2)}, \mathbf{b}^{(2)}, \mathbf{W}_{\text{pred}}, \mathbf{b}_{\text{pred}}$

- 1: set $i = 2, \alpha^{(2)} = \alpha, \tau^{(2)} = \tau, \gamma^{(2)} = \gamma$.
- 2: Minimize the loss function (2.5):

$$(2.5) \quad \min_{\substack{\mathbf{W}^{(1)}, \mathbf{b}^{(1)}; \\ \mathbf{W}^{(2)}, \mathbf{b}^{(2)}; \\ \mathbf{W}_{\text{pred}}, \mathbf{b}_{\text{pred}}}} \Phi_d \left(\mathbf{C}, h_{\text{pred}} \left(\mathbf{W}_{\text{pred}} \mathcal{R}^{(2)} \left(\mathbf{Y}^{(2)} \right) + \mathbf{b}_{\text{pred}} \right) \right) + \alpha^{(2)} \Phi_s \left(\mathbf{W}^{(1)}, \mathbf{b}^{(1)}, \mathbf{W}^{(2)}, \mathbf{b}^{(2)} \right) \\ + \tau^{(2)} \Phi_p \left(h_{\text{pred}} \left(\mathbf{W}_{\text{pred}} \mathcal{R}^{(2)} \left(\mathbf{Y}^{(2)} \right) + \mathbf{b}_{\text{pred}} \right) \right) + \gamma^{(2)} \Phi_m \left(\mathbf{Y}^{(2)} \right), \\ \text{subject to } \mathbf{Y}^{(2)} = \mathcal{R}^{(1)} \left(\mathbf{Y}^{(1)} \right) + h^{(2)} \left(\mathbf{W}^{(2)} \mathcal{R}^{(1)} \left(\mathbf{Y}^{(1)} \right) + \mathbf{b}^{(2)} \right), \\ \mathbf{Y}^{(1)} = h^{(1)} \left(\mathbf{W}^{(1)} \mathbf{X} + \mathbf{b}^{(1)} \right).$$

- 3: **Define:** $\eta^{(2)} =$ data loss after minimizing (2.5), $\varepsilon_v^{(2)} =$ val. loss, set $\eta^{(1)} \approx 0, \varepsilon_v^{(1)} > \varepsilon_v^{(2)}$.
- 4: **while** $\left| \frac{\eta^{(i-1)} - \eta^{(i)}}{\eta^{(i-1)}} \right| > \varepsilon_\eta$ **and** $\left[\varepsilon_v^{(i)} < \varepsilon_v^{(i-1)} \right]$ **do**
- 5: $i = i + 1$
- 6: Update $(\alpha^{(i)}, \tau^{(i)}, \gamma^{(i)})$ based on the previous values $(\alpha^{(i-1)}, \tau^{(i-1)}, \gamma^{(i-1)})$.
- 7: Extend the neural network by one layer with weights $\mathbf{W}^{(i)}$ and $\mathbf{b}^{(i)}$ initialized as zero.
- 8: Initialize \mathbf{W}_{pred} and \mathbf{b}_{pred} with values inherited from the previously trained network.
- 9: Freeze the weights $\mathbf{W}^{(1)}, \mathbf{b}^{(1)}, \{\mathbf{W}^{(l)}\}_{l=1}^{i-1}, \{\mathbf{b}^{(l)}\}_{l=1}^{i-1}$.
- 10: Minimize the loss function (2.6):

$$(2.6) \quad \min_{\substack{\mathbf{W}^{(i)}, \mathbf{b}^{(i)}; \\ \mathbf{W}_{\text{pred}}, \mathbf{b}_{\text{pred}}}} \Phi_d \left(\mathbf{C}, h_{\text{pred}} \left(\mathbf{W}_{\text{pred}} \mathcal{R}^{(i)} \left(\mathbf{Y}^{(i)} \right) + \mathbf{b}_{\text{pred}} \right) \right) + \alpha^{(i)} \times \Phi_s \left(\mathbf{W}^{(i)}, \mathbf{b}^{(i)} \right) \\ + \tau^{(i)} \times \Phi_p \left(h_{\text{pred}} \left(\mathbf{W}_{\text{pred}} \mathcal{R}^{(i)} \left(\mathbf{Y}^{(i)} \right) + \mathbf{b}_{\text{pred}} \right) \right) + \gamma^{(i)} \times \Phi_m \left(\mathbf{Y}^{(i)} \right), \\ \text{subject to } \mathbf{Y}^{(l+1)} = \mathcal{R}^{(l)} \left(\mathbf{Y}^{(l)} \right) + h^{(l+1)} \left(\mathbf{W}^{(l+1)} \mathcal{R}^{(l)} \left(\mathbf{Y}^{(l)} \right) + \mathbf{b}^{(l+1)} \right), \quad l = 1, \dots, i-1 \\ \mathbf{Y}^{(1)} = h^{(1)} \left(\mathbf{W}^{(1)} \mathbf{X} + \mathbf{b}^{(1)} \right).$$

- 11: Threshold weights, biases: if $|w_{jk}| < \rho$ then set $w_{jk} = 0$; if $|b_j| < \rho$ then set $b_j = 0$.
- 12: Store the training loss $\eta^{(i)}$ and corresponding best validation loss $\varepsilon_v^{(i)}$.
- 13: **end while**

Algorithm 2.2 Sequential residual learning

Input: Training data \mathbf{X} , labels \mathbf{C} , validation data \mathbf{X}_1 , validation labels \mathbf{C}_1 , trained network \mathcal{N} from Algorithm 2.1 and the corresponding validation loss $\varepsilon_v^{(1)}$, loss function Φ_d , training epoch E_e .

Initialize: Maximum number of networks: N_n , initialize each network: \mathcal{Q}_r with ≤ 2 hidden layers.

- 1: set $r = 1$, set $\varepsilon_v^{(0)} > \varepsilon_v^{(1)}$, $\mathcal{Q}_1 = \mathcal{N}$
- 2: **while** $r \leq N_n$ **and** $\left[\varepsilon_v^{(r)} < \varepsilon_v^{(r-1)} \right]$ **do**
- 3: Load trained network \mathcal{Q}_r
- 4: $\mathbf{C} = \mathbf{C} - \mathcal{Q}_r(\mathbf{X})$
- 5: Initialize network \mathcal{Q}_{r+1} with output layer parameters as 0.
- 6: Train network \mathcal{Q}_{r+1} for E_e epochs with data \mathbf{X} , labels \mathbf{C} and loss function Φ_d .
- 7: Restore the best network \mathcal{Q}_{r+1} , and validation loss $\varepsilon_v^{(r+1)}$.
- 8: $r = r + 1$
- 9: **end while**
- 10: Compute the net output as: $\mathbf{Y} = \mathcal{N}(\mathbf{X}) + \mathcal{Q}(\mathbf{X})$, where $\mathcal{Q}(\mathbf{X}) = \mathcal{Q}_2(\mathbf{X}) + \dots + \mathcal{Q}_{r-1}(\mathbf{X})$.

problem for each additional layer. Note that each layer of a deep neural network can be regarded as an ‘‘information filter’’ [29] transferring information from a previous layer to next layer. In particular, it is interesting to look at how regularizations defined in section 2.1 helps the layerwise training strategy. Further, it is also important to know the conditions under which each additional added layer is trainable. To that end, let us define the following:

Definition 3.1 (Input space and neural transfer map). *Let the input data lie on $\mathcal{M}^{(0)} \subset \mathbb{R}^S$ such that $\mathcal{M}^{(0)} = \bigcup_{j=1}^K \mathcal{M}_j^{(0)}$, where each $\mathcal{M}_j^{(0)}$ contains similar data points based on some predefined similarity measure. Further, let $C_j \subset \mathcal{M}_j^{(0)}$ be the associated training data clusters. We define the neural transfer map $\mathcal{N}^{(i)}$ with domain $\mathcal{M}^{(i-1)}$ as:*

$$(3.1) \quad \begin{aligned} \mathcal{N}^{(i)}(\mathbf{x}) &= h^{(i)}\left(\mathbf{W}^{(i)*}\mathbf{x} + \mathbf{b}^{(i)*}\right), \text{ for } i = 1 \text{ and,} \\ \mathcal{N}^{(i)}(\mathbf{x}) &= \mathbf{x} + h^{(i)}\left(\mathbf{W}^{(i)*}\mathbf{x} + \mathbf{b}^{(i)*}\right), \text{ for } i = 2, 3, \dots, L \end{aligned}$$

where $\mathbf{W}^{(i)*}$ and $\mathbf{b}^{(i)*}$ denote the trained biases and weights of the i^{th} layer, N_o represents the number of neurons in each hidden layer, and the domain $\mathcal{M}^{(i)}$ for each subsequent neural transfer map $\mathcal{N}^{(i+1)}$ is obtained as:

$$(3.2) \quad \mathcal{M}^{(i)} = \bigcup_{j=1}^K \mathcal{M}_j^{(i)}, \text{ where, } \mathcal{M}_j^{(i)} = \mathcal{R}^{(i)}\left(\mathcal{N}^{(i)}\left(\mathcal{M}_j^{(i-1)}\right)\right), \text{ for } i = 1, 2, \dots, L - 1$$

A key aspect of the algorithm is to learn transfer maps $\mathcal{N}^{(i)}$ that allows for effective information transfer through the network. In this work, we focus on creating transfer maps $\mathcal{N}^{(i)}$ that are

δ -stable for a given input \mathbf{x} through the use of manifold regularization [24, 7, 58]. A schematic of Algorithm 2.1 is given in Figure 1.

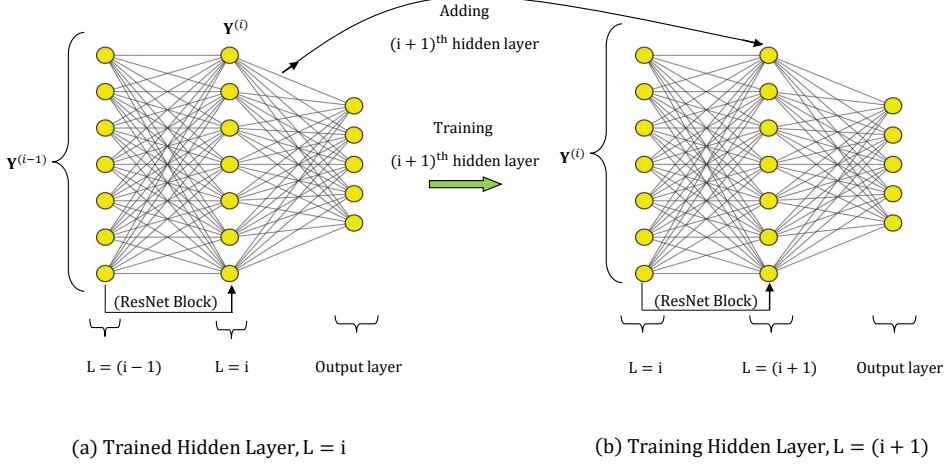


Figure 1. Schematic of Algorithm 2.1: Training the $(i + 1)^{\text{th}}$ hidden layer.

3.1.1. δ -stability in layerwise training Algorithm 2.1. In this section, we investigate the relevance of manifold regularization in our framework. The main motivation of manifold regularization is to promote δ -stability. Here, stability means if two data points are “similar” to each other in some sense, then the network predictions on the two data points must be close to each other. Thus, stability in this sense is closely related to continuity. We now provide the details.

Definition 3.2 ($\varepsilon - \delta$ stability promoting algorithm). Let $\mathcal{X} = \bigcup_{j=1}^K \mathcal{X}_j$ denote the input space, where each \mathcal{X}_j contains similar data points based on some assumed similarity measure. Consider a parameterized function $f_{\theta} : \mathcal{X} \subset \mathbb{R}^T \rightarrow \mathcal{Y}$ and a learning algorithm to find an “optimal” parameter θ^* . Let ζ be a stability parameter characteristic of the learning algorithm and let ε be a given constant. We call a learning algorithm to be $\varepsilon - \delta$ stability promoting algorithm for f_{θ} if there exists a stability function $\delta_j(\zeta) : [\zeta^l, \zeta^u] \rightarrow \mathbb{R}$, such that:

1. $\delta_j(\zeta^u) = \varepsilon$, $\delta_j(\zeta^u) < \delta_j(\zeta^l)$,
2. $\delta_j(\zeta)$ is continuous with respect to ζ ,
3. For each cluster \mathcal{X}_j , there exists $\theta^* = \theta^*(\zeta)$ such that:

$$(3.3) \quad \|f_{\theta^*}(\mathbf{x}) - f_{\theta^*}(\mathbf{x}')\|_2 \leq \delta_j(\zeta), \quad \forall \mathbf{x}, \mathbf{x}' \in \mathcal{X}_j.$$

Remark 3.3. Conditions 1, and 2 implies that the algorithm can promote any desired stability $\delta_{desired} \in (\varepsilon, \delta_j(\zeta^l))$ by varying parameter ζ , i.e $\exists \zeta^* \in (\zeta^l, \zeta^u)$ such that $\delta_j(\zeta^*) = \delta_{desired}$ (Intermediate value theorem). Note that ε is the best stability that can be achieved. However,

if the domain of $\delta_j(\zeta)$ is discrete, i.e, the hyperparameter ζ of the learning algorithm can only take discrete values in $[\zeta^l, \zeta^u]$, then we consider a relaxation of condition 2 in Definition 3.2. To that end we define “discrete $\varepsilon - \delta$ stability promoting algorithm” in Definition 3.4.

Definition 3.4 (Discrete $\varepsilon - \delta$ stability promoting algorithm). Consider Definition 3.2 and assume that the parameter ζ takes only discrete values, i.e $\zeta \in \{\zeta^l = \zeta_1, \zeta_2, \dots, \zeta_{n-1}, \zeta_n = \zeta^u\}$ and let the discrete domain of $\delta_j(\zeta)$ be denoted as D . Then, we call a learning algorithm to be discrete $\varepsilon - \delta$ stability promoting algorithm for f_{θ} if $\delta_j(\zeta) : D \rightarrow \mathbb{R}$ satisfies:

1. $\delta_j(\zeta^u) = \varepsilon, \delta_j(\zeta^u) < \delta_j(\zeta^l)$,
2. $\delta_j(\zeta)$ is monotonically decreasing with respect to ζ ,
3. For each cluster \mathcal{X}_j , there exists $\theta^* = \theta^*(\zeta)$ such that:

$$(3.4) \quad \|f_{\theta^*}(\mathbf{x}) - f_{\theta^*}(\mathbf{x}')\|_2 \leq \delta_j(\zeta), \quad \forall \mathbf{x}, \mathbf{x}' \in \mathcal{X}_j.$$

Remark 3.5. Conditions 3 in Definition 3.4 implies that the learning algorithm can continuously promote/improve the stability in a discrete manner by increasing ζ . However, the notion of discrete stability promoting algorithm in Definition 3.4 is weaker than the one in Definition 3.2 since it promotes only desired stability $\delta_{desired} \in \{\delta_j(\zeta_1), \delta_j(\zeta_2), \dots, \delta_j(\zeta_{n-1}), \delta_j(\zeta_n)\}$.

Definition 3.6 (δ -stable function). Consider the parameterized function f_{θ} and an $\varepsilon - \delta$ stability promoting algorithm as defined in Definition 3.2 or Definition 3.4. Let ζ^* be the optimal stability parameter chosen based on a predefined criteria. Then, we call the function f_{θ^*} to be $\delta_j(\zeta^*)$ -stable on \mathcal{X}_j (or in short δ -stable) if it satisfies (3.3).

Remark 3.7. In this work, the optimal ζ^* is defined as the one that minimizes the validation loss. That is, one looks at the performance on a validation data-set (exploring the balance between over-stabilization and under-stabilization) to pick ζ^* . A numerical demonstration in the context of choosing the best manifold regularization parameter is provided in subsection 4.1, Figure 2 (middle figure). Here, one plots the $(\zeta, \text{validation loss})$ curve and chooses ζ^* that gives the lowest validation loss. More details are provided in subsection 4.1.

For learning a δ -stable function in the sense of Definition 3.6, we first need to create an $\varepsilon - \delta$ stability promoting algorithm. To that end, we first determine the conditions under which one has an $\varepsilon - \delta$ stability promoting algorithm through the use of manifold regularization. For analysis purpose, let us first consider a re-normalization of the loss (2.6) as follows:

$$(3.5) \quad \mathcal{L}_r = (\gamma^u - \gamma^{(i)}) \times \Phi_d + (\gamma^u - \gamma^{(i)}) \alpha^{(i)} \times \Phi_s + (\gamma^u - \gamma^{(i)}) \tau^{(i)} \times \Phi_p + \gamma^{(i)} \times \Phi_m,$$

where γ^u is a predefined upper bound such that when $\gamma^{(i)} = \gamma^u$, Φ_m (manifold regularization) is the sole component in the total loss \mathcal{L}_r , and when $\gamma^{(i)} = 0$, the manifold regularization is absent. Now, we are in the position to show the existence of a stability function when employing manifold regularization. To that end we will first prove the following lemma.

Lemma 3.8 (Set of minimizers $\theta^*(\gamma^{(i)})$ is upper hemicontinuous with respect to $\gamma^{(i)}$). Consider the loss (3.5) associated with training the layer $\mathcal{N}^{(i)}$. For a given $\{\alpha^{(i)}, \tau^{(i)}\}$ we define the loss function (3.5) as $\Phi(\theta, \gamma^{(i)})$, where θ represents the weights and biases to be optimized.

Suppose the set of global minimizers, $S(\gamma^{(i)}) = \{\theta^* : \theta^* = \arg \min_{\theta} \Phi(\theta, \gamma^{(i)})\}$ corresponding to the loss function (2.6) is non-empty and commonly bounded¹ for all $\gamma^{(i)} \in [0, \gamma^u]$, where γ^u is a predefined upper bound. Then, $S(\gamma^{(i)})$ is upper hemicontinuous in $\gamma^{(i)}$.

Proof. We shall use the Berge maximum theorem (refer to Chapter 17 in [8]) to show that the set of minimizers $S(\gamma^{(i)})$ is upper hemicontinuous with respect to $\gamma^{(i)}$. To that end the following observations can be made:

1. $\Phi(\theta, \gamma^{(i)})$ is continuous with respect to both θ and $\gamma^{(i)}$, since each component of the total loss (3.5) is continuous.
2. Let \mathbb{R}^c be the Euclidean space with c being the total number of parameters and $\mathcal{P}(\mathbb{R}^s)$ be the set of all subsets of \mathbb{R}^s . There exists a compact-valued correspondence $C : [0, \gamma^u] \rightarrow \mathcal{P}(\mathbb{R}^s)$ with $C(\gamma^{(i)}) \neq \emptyset, \forall \gamma^{(i)} \in [0, \gamma^u]$ such that:

$$\theta^*(\gamma^{(i)}) = \arg \min_{\theta \in C(\gamma^{(i)})} \Phi(\theta, \gamma^{(i)}) = \arg \min_{\theta \in \mathbb{R}^c} \Phi(\theta, \gamma^{(i)}).$$

Indeed, since the set of global minimizers is non-empty $\forall \gamma^{(i)} \in [0, \gamma^u]$, the existence of a compact-valued correspondence is straightforward to verify by defining the constraint set to be the same for each $\gamma^{(i)} \in [0, \gamma^u]$, i.e $C(\gamma^{(i)}) = \overline{\bigcup_{\gamma^{(j)} \in [0, \gamma^u]} S(\gamma^{(j)})}$, where $\overline{(\cdot)}$ denotes the closure of the set. Further, $C(\gamma^{(i)})$ is closed and bounded, and hence compact, due to the assumption that the set of global minimizers is commonly bounded $\forall \gamma^{(i)} \in [0, \gamma^u]$,

3. Since the compact constraint set $C(\gamma^{(i)})$ defined above is constant independent of $\gamma^{(i)}$, it is continuous (refer to Chapter 17 in [8]).

Thus, by Berge maximum theorem the correspondence $\theta^*(\gamma^{(i)})$ is upper hemicontinuous with respect to $\gamma^{(i)}$.

Proposition 3.9 ($\varepsilon - \delta$ stability promoting algorithm via manifold regularization). Consider the input space and neural transfer map introduced in Definition 3.1. Further assume that:

1. The samples in cluster C_p^2 are independent draws from $\mu_p^{(0)}$ with support $\mathcal{M}_p^{(0)} \subset \mathcal{M}^{(0)}$ where $\mathcal{M}_p^{(0)}$ is compact $\forall p$. Let $\mu_p^{(i)} = (\mathcal{R}^{(i)} \mathcal{N}^{(i)})_{\#} \mu_p^{(i-1)}$ be the push forward measure associated with the map (3.2) for $i = 1, \dots$.
2. The linear transformation $\mathcal{R}^{(i)}$ in (3.2) rescales the features to $[-M, 0]$, where M is a positive number and the activation $h^{(i)} \in \{\text{ELU}, \text{ReLU}, \text{LeakyReLU}, \text{SELU}\}$ for $i = 2, \dots, L$.
3. The set $S(\gamma^{(i)})$ in lemma 3.8 is singleton $\forall \gamma^{(i)} \in [0, \gamma^u]$. That is, the global minimizer is unique $\forall \gamma^{(i)} \in [0, \gamma^u]$ and for any choice of β_p in (2.3).

Then, employing manifold regularization Φ_m of the form (2.4) with $\beta_p = 1, \forall p$ yields a probabilistic $\varepsilon - \delta$ stability promoting algorithm for $\mathcal{N}^{(i+1)}$. In particular, there exists a stability function $\tilde{\delta}_p(\gamma^{(i)}, \xi^{(i)}) : [0, \gamma^u] \times (0, 1) \rightarrow \mathbb{R}$, that satisfies conditions 1 and 2 for every given

¹Commonly bounded means that $\exists M < \infty$, independent of $\gamma^{(i)}$, such that $\sup_{\gamma^{(i)} \in [0, \gamma^u]} |\theta^*(\gamma^{(i)})| \leq M$.

²Note that we do not assume that labels are available for all the inputs.

$\xi^{(i)}$, such that $\forall \mathbf{x}, \mathbf{x}'$ in $\mathcal{M}_p^{(i-1)}$:

$$(3.6) \quad \left\| \mathcal{N}^{(i)}(\mathbf{x}) - \mathcal{N}^{(i)}(\mathbf{x}') \right\|_2^2 \leq \tilde{\delta}_p \left(\gamma^{(i)}, \xi^{(i)} \right), \quad i = 2, \dots, L,$$

holds with probability at-least $\left(1 - \xi^{(i)} - \mathcal{E}_p^{(i)}(m_p, \xi^{(i)}\varepsilon) \right)$, where $\mathcal{M}_p^{(i-1)}$ is defined in (3.2), $\gamma^{(i)}$ is the weight associated with the manifold regularization term in (2.6), $\mathcal{E}_p^{(i)}(m_p, \varepsilon) = 2m_p \exp\left(-\omega_p^{(i)} m_p \varepsilon^2\right) + 2 \exp\left(-\vartheta_p^{(i)} m_p \varepsilon^2\right)$, and $\omega_p^{(i)}, \vartheta_p^{(i)}$ are positive constants that depends only on the cluster C_p and the layer i .

Proof. The proof follows directly from analyzing the effect of manifold regularization applied to each neural transfer map. Consider the trained neural transfer map $\mathcal{N}^{(2)}(\mathbf{x})$ which is the hidden layer of the ResNet architecture after the upsampling/downsampling layer. From (2.4) with $\beta_p = 1, \forall p$, a sample average approximation of the manifold regularization term Φ_m can be written as:

$$(3.7) \quad \sum_{p=1}^K \left[\frac{1}{m_p^2} \sum_{\mathbf{x}_i, \mathbf{x}_j \in C_p} \left\| \mathcal{N}^{(2)}(\mathbf{x}_i) - \mathcal{N}^{(2)}(\mathbf{x}_j) \right\|_2^2 \right],$$

where, m_p denotes the number of data points in cluster C_p , and $C_1, C_2 \dots C_k$ denotes the data clusters. Now for each cluster C_p , one can show the following non-asymptotic bound (proof is provided in Appendix A):

$$(3.8) \quad \mathbb{P} \left[\mathbb{E}_{\mu_p^{(1)}} \left[\left\| \mathcal{N}^{(2)}(\mathbf{x}) - \mathcal{N}^{(2)}(\mathbf{y}) \right\|_2^2 \right] \leq \varepsilon + \frac{1}{m_p^2} \sum_{\mathbf{x}_i, \mathbf{x}_j \in C_p} \left\| \mathcal{N}^{(2)}(\mathbf{x}_i) - \mathcal{N}^{(2)}(\mathbf{x}_j) \right\|_2^2 \right] \geq \mathcal{E}_p^{(2)}(m_p, \varepsilon),$$

$$(3.9) \quad \mathbb{E}_{\mu_p^{(1)}} \left[\left\| \mathcal{N}^{(2)}(\mathbf{x}) - \mathcal{N}^{(2)}(\mathbf{y}) \right\|_2^2 \right] = \int_{\mathcal{M}_p^{(1)}} \int_{\mathcal{M}_p^{(1)}} \left\| \mathcal{N}^{(2)}(\mathbf{x}) - \mathcal{N}^{(2)}(\mathbf{y}) \right\|_2^2 d\mu_p^{(1)}(\mathbf{x}) d\mu_p^{(1)}(\mathbf{y}).$$

where $\mathcal{E}_p^{(2)}(m_p, \varepsilon) = 1 - 2m_p \exp\left(-\omega_p^{(2)} m_p \varepsilon^2\right) - 2 \exp\left(-\vartheta_p^{(2)} m_p \varepsilon^2\right)$, $\omega_p^{(2)}, \vartheta_p^{(2)}$ are positive constants that depends only on the cluster C_p and the hidden layer, and \mathbb{E}_{μ_p} is the expectation defined in (3.9). Now, note that the random variable $\left\| \mathcal{N}^{(2)}(\mathbf{x}) - \mathcal{N}^{(2)}(\mathbf{y}) \right\|_2^2$ in (3.9) is non-negative. Therefore, by Markov inequality [52] we have:

$$(3.10) \quad \left\| \mathcal{N}^{(2)}(\mathbf{x}) - \mathcal{N}^{(2)}(\mathbf{x}') \right\|_2^2 \leq \frac{\mathbb{E}_{\mu_p^{(1)}} \left[\left\| \mathcal{N}^{(2)}(\mathbf{x}) - \mathcal{N}^{(2)}(\mathbf{y}) \right\|_2^2 \right]}{\xi^{(2)}},$$

holds $\forall \mathbf{x}, \mathbf{x}'$ on $\mathcal{M}_p^{(1)}$ with probability at-least $(1 - \xi^{(2)})$. Now using the non-asymptotic bound (3.8) in (3.10) and applying the union bound, we have:

$$(3.11) \quad \left\| \mathcal{N}^{(2)}(\mathbf{x}) - \mathcal{N}^{(2)}(\mathbf{x}') \right\|_2^2 \leq \frac{1}{\xi^{(2)} \times m_p^2} \sum_{\mathbf{x}_i, \mathbf{x}_j \in C_p} \left\| \mathcal{N}^{(2)}(\mathbf{x}_i) - \mathcal{N}^{(2)}(\mathbf{x}_j) \right\|_2^2 + \varepsilon,$$

holds $\forall \mathbf{x}, \mathbf{x}'$ on $\mathcal{M}_p^{(1)}$ with probability at-least $(1 - \xi^{(2)} - \mathcal{E}_p^{(2)}(m_p, \xi^{(2)}\varepsilon))$. Therefore, from (3.11) the stability function $\tilde{\delta}_p(\gamma^{(2)}, \xi^{(2)})$ is defined as follows:

$$(3.12) \quad \tilde{\delta}_p(\gamma^{(2)}, \xi^{(2)}) = \frac{1}{\xi^{(2)} \times m_p^2} \sum_{\mathbf{x}_i, \mathbf{x}_j \in C_p} \left\| \mathcal{N}_{\boldsymbol{\theta}^*(\gamma^{(2)})}^{(2)}(\mathbf{x}_i) - \mathcal{N}_{\boldsymbol{\theta}^*(\gamma^{(2)})}^{(2)}(\mathbf{x}_j) \right\|_2^2 + \varepsilon,$$

where we have introduced the subscript $\boldsymbol{\theta}^*(\gamma^{(2)})$ to denote the optimal weights and biases of the trained layer $\mathcal{N}^{(2)}$ and $\xi^{(2)} \in (0, 1)$. We will first prove that (3.12) is a valid stability function that satisfies condition 1 and condition 2 in Definition 3.2 for every choice of $\xi^{(2)}$. Condition 1 is satisfied by setting $\gamma^{(2)} = \gamma^u$ in (3.5), since manifold regularization is the sole component in the total loss and consequently (3.7) is minimized. The minimizers in this case can be identified by noticing that:

$$(3.13) \quad \begin{aligned} & \left\| \mathcal{N}_{\boldsymbol{\theta}^*(\gamma^{(2)})}^{(2)}(\mathbf{x}_i) - \mathcal{N}_{\boldsymbol{\theta}^*(\gamma^{(2)})}^{(2)}(\mathbf{x}_j) \right\|_2^2 = \\ & \left\| \mathbf{x}_i - \mathbf{x}_j + h^{(2)}\left(\mathbf{W}^{(2)*}\mathbf{x}_i + \mathbf{b}^{(2)*}\right) - h^{(2)}\left(\mathbf{W}^{(2)*}\mathbf{x}_j + \mathbf{b}^{(2)*}\right) \right\|_2^2, \end{aligned}$$

which follows from (3.1). Based on assumption 2, we immediately notice that the minimizers are $\mathbf{b}^{(2)*} = 0$ and $\mathbf{W}^{(2)*} = (-\lambda) \times \mathcal{I}$, where \mathcal{I} is the identity matrix and λ is a constant depending on the activation function employed. In this case, the minimizers $\mathbf{b}^{(2)*}$, $\mathbf{W}^{(2)*}$ leads to the network learning a zero function and $\tilde{\delta}_p(\gamma^u, \xi^{(2)}) = \varepsilon$, $\forall p$ in (3.12). Now since the minimizers $\mathbf{b}^{(2)*}$, $\mathbf{W}^{(2)*}$ is unique for any choice of similarity matrix $\boldsymbol{\beta}$ in (2.3) (assumption 3), we also note that $\tilde{\delta}_p(\gamma^u, \xi^{(2)}) = \varepsilon$ for any p if and only if the network learns a zero function. Therefore, by contraposition it follows that $\forall p$, $\tilde{\delta}_p(0, \xi^{(2)}) > \varepsilon$ since in the absence of manifold regularization term (i.e $\gamma^{(2)} = 0$), it is necessary that the hidden layers learns a non-zero function to fit the training data. In conclusion, we have proved the following properties for $\tilde{\delta}_p(\gamma^{(2)}, \xi^{(2)})$:

$$(3.14) \quad \tilde{\delta}_p(\gamma^u, \xi^{(2)}) = \varepsilon, \quad \tilde{\delta}_p(0, \xi^{(2)}) > \varepsilon, \quad \forall p.$$

Now, in order to prove condition 2 of Definition 3.2, it is sufficient to show that $\tilde{\delta}_p(\gamma^{(2)}, \xi^{(2)})$ is continuous with respect to $\gamma^{(2)}$. Note that, $\forall \gamma^{(2)} \in [0, \gamma^u]$ we have:

(3.15a)

$$\lim_{r \rightarrow 0} \tilde{\delta}_p(r + \gamma^{(2)}, \xi^{(2)}) = \lim_{r \rightarrow 0} \left[\frac{1}{\xi^{(2)} \times m_p^2} \sum_{\mathbf{x}_i, \mathbf{x}_j \in C_p} \left\| \mathcal{N}_{\boldsymbol{\theta}^*(r + \gamma^{(2)})}^{(2)}(\mathbf{x}_i) - \mathcal{N}_{\boldsymbol{\theta}^*(r + \gamma^{(2)})}^{(2)}(\mathbf{x}_j) \right\|_2^2 \right] + \varepsilon$$

$$(3.15b) \quad = \frac{1}{\xi^{(2)} \times m_p^2} \left[\sum_{\mathbf{x}_i, \mathbf{x}_j \in C_p} \lim_{r \rightarrow 0} \left\| \mathcal{N}_{\boldsymbol{\theta}^*(r + \gamma^{(2)})}^{(2)}(\mathbf{x}_i) - \mathcal{N}_{\boldsymbol{\theta}^*(r + \gamma^{(2)})}^{(2)}(\mathbf{x}_j) \right\|_2^2 \right] + \varepsilon$$

$$(3.15c) \quad = \frac{1}{\xi^{(2)} \times m_p^2} \sum_{\mathbf{x}_i, \mathbf{x}_j \in C_p} \left\| \mathcal{N}_{\boldsymbol{\theta}^*(\gamma^{(2)})}^{(2)}(\mathbf{x}_i) - \mathcal{N}_{\boldsymbol{\theta}^*(\gamma^{(2)})}^{(2)}(\mathbf{x}_j) \right\|_2^2 + \varepsilon$$

$$(3.15d) \quad = \tilde{\delta}_p(\gamma^{(2)}, \xi^{(2)})$$

where we have used the fact that $\theta^*(\gamma^{(2)})$ is a continuous function in (3.15c) based on assumption 3 and using the results of lemma 3.8. Therefore, condition 2 of Definition 3.2 is satisfied. Now, applying the above arguments for δ -stability recursively for subsequent neural transfer maps $\mathcal{N}^{(i)}$, it follows that property (3.6) holds for any subsequent neural transfer maps $\mathcal{N}^{(i)}$, thereby concluding the proof.

Remark 3.10. In order to reduce the number of hyperparameters, we consider a fixed growth/decay rate for the manifold regularization weight, i.e. $\gamma^{(i+1)} = \kappa\gamma^{(i)}$ in (3.5). When $\kappa \in (0, 1)$, more emphasis is placed on minimizing the data loss Φ_d in the later layers while the initial layers focus on stability. This strategy is suitable for regression/classification task with sufficient number of data points as demonstrated in subsection 4.1 and subsection 4.4. However, when the data set is sparse we consider choosing a small value for $\gamma^{(2)}$ and $\kappa > 1$ such that the initial layers over-fits on the sparse data set and stability is imparted in the later layers. The feasibility of such a training procedure for sparse data sets is discussed in subsection 4.3.1. *In either case, this leads to tuning only parameter $\gamma^{(2)}$ in our procedure. Corollary 3.11 below shows that employing manifold regularization in this way yields an $\varepsilon - \delta$ stability promoting algorithm for the entire network \mathcal{N} .* In Corollary 3.11, we also look at the asymptotic behavior when $m_p \rightarrow \infty$, i.e one has access to unlimited training data points in each cluster.

Corollary 3.11. *Assume that conditions in Proposition 3.9 are satisfied and each cluster contains infinitely many samples. Further, assume that the activation function employed is Lipschitz continuous and assume $\gamma^{(i+1)} = \kappa\gamma^{(i)}$ in (3.5), where κ is a fixed growth/decay rate for the manifold regularization weight. Then, employing manifold regularization of the form (2.4) with $\beta_p = 1, \forall p$ yields a probabilistic $\varepsilon - \delta$ stability promoting algorithm for network \mathcal{N} with $\varepsilon = 0$ in the sense of Definition 3.2. That is, there exists a stability function $\delta_p^{\mathcal{N}}(\gamma, \xi^{(2)}, \dots, \xi^{(L)}) : [0, \gamma^u] \times (0, 1)^{L-1} \rightarrow \mathbb{R}$ that satisfies conditions 1 and 2 for any fixed $\xi^{(2)}, \dots, \xi^{(L)}$, such that in the limit $m_p \rightarrow \infty^3, \forall \mathbf{x}, \mathbf{x}' \in \mathcal{M}_p^{(0)} \subset \mathcal{M}^{(0)}$:*

$$(3.16) \quad \|\mathcal{N}(\mathbf{x}) - \mathcal{N}(\mathbf{x}')\|_2^2 \leq \delta_p^{\mathcal{N}}(\gamma, \xi^{(2)}, \dots, \xi^{(L)}),$$

holds with probability at-least $(1 - \sum_{i=2}^L \xi^{(i)})$, where $\gamma = \gamma^{(2)}$ is the initial weight chosen for the manifold regularization term in the loss (3.5).

Proof. Proof is provided in Appendix B.

Remark 3.12. Note that for a given $\xi^{(2)}, \dots, \xi^{(L)}$, the stability function $\delta_p^{\mathcal{N}}(\gamma, \xi^{(2)}, \dots, \xi^{(L)})$ can be made as small as one wishes by varying the parameter γ (also see remark 3.3). A numerical demonstration of controlling the stability function by varying γ is provided in Figure 7 of subsection 4.3. Further, by choosing the optimal stability parameter γ^* in (3.16), we achieve a δ -stable network \mathcal{N} in the sense of Definition 3.6.

3.1.2. Layerwise training saturation problem. Even though we have ensured that Algorithm 2.1 promotes $\varepsilon - \delta$ stability, it is imperative to analyse any training saturation problem

³Inequality (3.16) is an asymptotic property here. For more details, refer to the proof in Appendix B.

that might arise from certain hyperparameter settings. In this section, we consider the case when $\kappa \in (0, 1)$ in [Corollary 3.11](#) and derive the necessary conditions for trainability of a newly added layer (see [Proposition 3.15](#)). To that end, let us define the following:

Definition 3.13. *Layerwise training promoting property (LTP)*

A non-linear activation function $h(\cdot)$ possesses the layerwise training promoting property (LTP) if $h'(0) \neq 0$.

Definition 3.14. *Trainability of an added layer*

A newly added $(i+1)^{\text{th}}$ layer with parameters $\mathbf{W}^{(i+1)}$ and $\mathbf{b}^{(i+1)}$ initialized as \mathbf{W}_0 and \mathbf{b}_0 , respectively, is trainable with respect to the j^{th} training pair $\{\mathbf{Y}_j^{(i)}, \mathbf{C}_j\}$ if

$$\left[\frac{\partial \mathcal{L}_j}{\partial \mathbf{W}^{(i+1)}} \right]_{\mathbf{W}^{(i+1)}=\mathbf{W}_0} \neq \mathbf{0}, \quad \left[\frac{\partial \mathcal{L}_j}{\partial \mathbf{b}^{(i+1)}} \right]_{\mathbf{b}^{(i+1)}=\mathbf{b}_0} \neq \mathbf{0},$$

where \mathcal{L}_j is the Lagrangian defined for the j^{th} training sample in [\(C.3\)](#) in [Appendix C](#).

Proposition 3.15 (Necessary condition for trainability of newly added layer). Consider training the $(i+1)^{\text{th}}$ hidden layer with the loss [\(2.6\)](#) and parameters $\mathbf{W}^{(i+1)}$ and $\mathbf{b}^{(i+1)}$ initialized as zero and assume that $h^{(i+1)}(0) = 0$ and $\alpha^{(i)} = \alpha^{(i+1)} = 0$ (sparsity regularization). Further, assume that the i^{th} hidden layer is trained to a local minimum with respect to the j^{th} training sample such that $(h^{(i)})' \left(\mathbf{W}^{(i)*} \mathcal{R}^{(i-1)} \left(\mathbf{Y}_j^{(i-1)} \right) + \mathbf{b}^{(i)*} \right) \neq \mathbf{0}$, where $\mathbf{W}^{(i)*}$ and $\mathbf{b}^{(i)*}$ denote the optimal weights and biases of the i^{th} layer and $\mathcal{R}^{(i)}$ follows [assumption \(2\)](#). Then, the necessary conditions for trainability of an added layer are:

1. $\gamma^{(i+1)} \neq \gamma^{(i)}$ or $\tau^{(i+1)} \neq \tau^{(i)}$;
2. Activation $h^{(i+1)}$ should satisfy the LTP property.

Proof. The ResNet forward propagation (see [\(2.1\)](#)) for the newly added layer with weights and biases initialized as zero gives:

$$(3.17) \quad \mathbf{Y}^{(i+1)} = \mathcal{R}^{(i)} \left(\mathbf{Y}^{(i)} \right) + h^{(i+1)} \left(\mathbf{0} \times \mathcal{R}^{(i)} \left(\mathbf{Y}^{(i)} \right) + \mathbf{0} \right).$$

Since $h^{(i+1)}(0) = 0$, we have $\mathbf{Y}^{(i+1)} = \mathcal{R}^{(i)} \left(\mathbf{Y}^{(i)} \right)$ on adding the new layer at the beginning of training and the network output $h_{\text{pred}} \left(\mathbf{W}_{\text{pred}} \mathcal{R}^{(i+1)} \left(\mathbf{Y}^{(i+1)} \right) + \mathbf{b}_{\text{pred}} \right)$ remains unchanged since $\mathcal{R}^{(i+1)} \mathcal{R}^{(i)} \left(\mathbf{Y}^{(i)} \right) = \mathcal{R}^{(i)} \left(\mathbf{Y}^{(i)} \right)$, which follows from [assumption \(2\)](#). Now, using [\(3.17\)](#), the gradient for the newly added layer evaluated at $\mathbf{0}$ for a particular j^{th} training sample can be written as (see [Appendix C](#)):

$$(3.18) \quad \frac{\partial \mathcal{L}_j}{\partial \mathbf{b}^{(i+1)}} = - \left(\mathbf{R}^{(i)} \left(\mathbf{W}_{\text{pred}}^* \right)^T \left[h'_{\text{pred}} \left(\mathbf{W}_{\text{pred}}^* \mathcal{R}^{(i)} \left(\mathbf{Y}_j^{(i)} \right) + \mathbf{b}_{\text{pred}}^* \right) \circ \boldsymbol{\lambda}_2^{(i+1)} \right] - \frac{\partial \Phi_m^{(i+1)}}{\partial \mathbf{Y}_j^{(i)}} \right) \circ \left(h^{(i+1)} \right)'(\mathbf{0}),$$

and,

$$(3.19) \quad \frac{\partial \mathcal{L}_j}{\partial \mathbf{W}^{(i+1)}} = \frac{\partial \mathcal{L}_j}{\partial \mathbf{b}^{(i+1)}} \left(\mathcal{R}^{(i)} \left(\mathbf{Y}_j^{(i)} \right) \right)^T,$$

where \mathcal{L}_j denotes the Lagrangian defined in [Appendix C](#), (C.3), $\mathbf{W}_{\text{pred}}^*$, $\mathbf{b}_{\text{pred}}^*$ represents the optimal parameters for the output layer obtained after training the i^{th} layer, and $\lambda_2^{(i+1)}$ is defined as:

$$(3.20) \quad \lambda_2^{(i+1)} = - \left(\frac{\partial \Phi_d}{\partial \mathbf{Y}_j^{(o)}} + \frac{\partial \Phi_p^{(i+1)}}{\partial \mathbf{Y}_j^{(o)}} \right).$$

where, $\mathbf{Y}_j^{(o)}$ represents the output of the network. Therefore, it is clear from (3.18) that $(h^{(i+1)})'(\mathbf{0}) \neq 0$ (LTP property) is a necessary condition for trainability of the newly added layer. Further, since the previous layer, i.e the i^{th} layer is trained to a local minima, then one also has the following condition (see [Appendix C](#) equation (C.6)):

$$(3.21) \quad \left(\mathbf{R}^{(i)}(\mathbf{W}_{\text{pred}}^*)^T \left[h'_{\text{pred}} \left(\mathbf{W}_{\text{pred}}^* \mathcal{R}^{(i)} \left(\mathbf{Y}_j^{(i)} \right) + \mathbf{b}_{\text{pred}}^* \right) \circ \lambda_2^{(i)} \right] - \frac{\partial \Phi_m^i}{\partial \mathbf{Y}_j^{(i)}} \right) \circ \mathbf{z} = \mathbf{0},$$

where, $\mathbf{W}^{(i)*}$, $\mathbf{b}^{(i)*}$ denotes the trained parameters of the i^{th} layer and the vector \mathbf{z} given by:

$$\mathbf{z} = \left(h^{(i)} \right)' \left(\mathbf{W}^{(i)*} \mathcal{R}^{(i-1)} \left(\mathbf{Y}_j^{(i-1)} \right) + \mathbf{b}^{(i)*} \right) \neq \mathbf{0},$$

by assumption in [Proposition 3.15](#). Therefore, condition (3.21) translates to the following:

$$(3.22) \quad \frac{\partial \Phi_m^i}{\partial \mathbf{Y}_j^{(i)}} = \mathbf{R}^{(i)}(\mathbf{W}_{\text{pred}}^*)^T \left[h'_{\text{pred}} \left(\mathbf{W}_{\text{pred}}^* \mathcal{R}^{(i)} \left(\mathbf{Y}_j^{(i)} \right) + \mathbf{b}_{\text{pred}}^* \right) \circ \lambda_2^{(i)} \right].$$

Further from (3.20), we have:

$$(3.23) \quad \lambda_2^{(i+1)} = \lambda_2^{(i)} + \frac{\partial \Phi_p^i}{\partial \mathbf{Y}_j^{(o)}} - \frac{\partial \Phi_p^{(i+1)}}{\partial \mathbf{Y}_j^{(o)}}.$$

In addition from (3.18), for trainability of the newly added layer it is necessary that:

$$\mathbf{R}^{(i)}(\mathbf{W}_{\text{pred}}^*)^T \left[h'_{\text{pred}} \left(\mathbf{W}_{\text{pred}}^* \mathcal{R}^{(i)} \left(\mathbf{Y}_j^{(i)} \right) + \mathbf{b}_{\text{pred}}^* \right) \circ \lambda_2^{(i+1)} \right] - \frac{\partial \Phi_m^{(i+1)}}{\partial \mathbf{Y}_j^{(i)}} \neq \mathbf{0}.$$

The above condition can be simplified using (3.22), and (3.23) as:

$$(3.24) \quad \frac{\partial \Phi_m^i}{\partial \mathbf{Y}_j^{(i)}} - \frac{\partial \Phi_m^{(i+1)}}{\partial \mathbf{Y}_j^{(i)}} + \mathbf{R}^{(i)}(\mathbf{W}_{\text{pred}}^*)^T \left[h'_{\text{pred}} \left(\mathbf{W}_{\text{pred}}^* \mathcal{R}^{(i)} \left(\mathbf{Y}_j^{(i)} \right) + \mathbf{b}_{\text{pred}}^* \right) \circ \left(\frac{\partial \Phi_p^i}{\partial \mathbf{Y}_j^{(o)}} - \frac{\partial \Phi_p^{(i+1)}}{\partial \mathbf{Y}_j^{(o)}} \right) \right] \neq \mathbf{0}.$$

Using the (C.1) in [Appendix C](#), the above condition translates to:

$$(3.25) \quad \left(\gamma^{(i)} - \gamma^{(i+1)} \right) \frac{\partial \Phi_m}{\partial \mathbf{Y}_j^{(i)}} + \left(\tau^{(i)} - \tau^{(i+1)} \right) (\mathbf{W}_{\text{pred}}^*)^T \left[h'_{\text{pred}} \left(\mathbf{Y}_j^{(i)} \mathbf{W}_{\text{pred}}^* + \mathbf{b}_{\text{pred}}^* \right) \circ \frac{\partial \Phi_p}{\partial \mathbf{Y}_j^{(o)}} \right] \neq \mathbf{0}.$$

Thus, it is necessary that $\gamma^{(i+1)} \neq \gamma^{(i)}$ or $\tau^{(i+1)} \neq \tau^{(i)}$ for trainability.

Corollary 3.16 (Training saturation). *Assume that the necessary conditions of Proposition 3.15 are satisfied, by choosing $\gamma^{(i+1)} = \kappa_1 \gamma^{(i)}$ and $\tau^{(i+1)} = \kappa_2 \tau^{(i)}$, where $\kappa_1, \kappa_2 \in (0, 1)$. Then*

$$\lim_{i \rightarrow \infty} \frac{\partial \mathcal{L}_j}{\partial \mathbf{b}^{(i+1)}} = \mathbf{0}, \quad \text{and} \quad \lim_{i \rightarrow \infty} \frac{\partial \mathcal{L}_j}{\partial \mathbf{W}^{(i+1)}} = \mathbf{0},$$

for all $j = 1, \dots, M$.

Proof. Since the i^{th} layer is supposed to be trained to a local minimum with respect to each training sample, we have:

$$\left[\frac{\partial \mathcal{L}_j}{\partial \mathbf{b}^{(i)}} \right]_{\mathbf{b}^{(i)} = \mathbf{b}^{(i)*}} = \mathbf{0}, \quad \left[\frac{\partial \mathcal{L}_j}{\partial \mathbf{W}^{(i)}} \right]_{\mathbf{W}^{(i)} = \mathbf{W}^{(i)*}} = \mathbf{0}, \quad \forall j = 1, \dots$$

where, $\mathbf{W}^{(i)*}$ and $\mathbf{b}^{(i)*}$ denote the optimal parameters of the i^{th} layer. Since $\lim_{i \rightarrow \infty} |\gamma^{(i+1)} - \gamma^{(i)}| = 0$, $\lim_{i \rightarrow \infty} |\tau^{(i+1)} - \tau^{(i)}| = 0$, it follows from (3.25) and (3.18) that:

$$\left[\frac{\partial \mathcal{L}_j}{\partial \mathbf{W}^{(i+1)}} \right]_{\mathbf{W}^{(i+1)} = \mathbf{0}} \rightarrow \mathbf{0}, \quad \left[\frac{\partial \mathcal{L}_j}{\partial \mathbf{b}^{(i+1)}} \right]_{\mathbf{b}^{(i+1)} = \mathbf{0}} \rightarrow \mathbf{0}, \quad \forall j = 1, \dots, M.$$

as i approaches ∞ .

Remark 3.17. The results of Corollary 3.16 implies that for sufficiently large i , both $\frac{\partial \mathcal{L}_j}{\partial \mathbf{b}^{(i+1)}}$ and $\frac{\partial \mathcal{L}_j}{\partial \mathbf{W}^{(i+1)}}$ are small. In other words, we face the problem of vanishing gradient when adding new layer and the training saturates, i.e., either little or no decrease in the total loss given by (2.6) for sufficiently large i .

Remark 3.18. Note that we have assumed $h^{(i)}(0) = 0$ in Proposition 3.15. Further, the LTP property is a necessary condition for trainability of an added layer. It is easy to see that activation function such as ‘ELU’ and ‘Tanh’ satisfy these conditions. In addition, activation functions such as {ReLU[12], LeakyReLU, SELU} can also be used in practice if one considers a non-zero subgradient at 0. In this work, the activation functions $h^{(i)}$ in Algorithm 2.1 are selected to be ELU.

3.2. Sequential residual learning Algorithm 2.2. Recall that promoting $\varepsilon - \delta$ stability (Corollary 3.11) does not guarantee that the network classifies/regress correctly since training saturates for certain hyperparameter settings in Algorithm 2.1 (see Corollary 3.16). To overcome this issue, we incorporate a post-processing stage termed as the “*sequential residual learning*” step for further improving the predictions. The idea of sequential residual learning is to train a sequence of shallow neural networks to learn the residual (i.e lower the data loss Φ_d while generalizing well) from Algorithm 2.1 where each network \mathcal{Q}_i is trained for a limited epochs to prevent overfitting on the residuals. Algorithm 2.2 creates new training problem for each network \mathcal{Q}_{i+1} by generating data sets of the form:

$$(3.26) \quad \mathcal{K}_{II,i+1} = \{ \mathbf{X}, \mathbf{C}_i \}, \quad \mathbf{C}_i = \mathbf{C}_{i-1} - \mathcal{Q}_i(\mathbf{X}), \quad i = 1, 2, \dots$$

where, $\mathbf{C}_0 = \mathbf{C}$ and $\mathcal{Q}_1 = \mathcal{N}$ is the neural network produced by Algorithm 2.1. For a given test data point \mathbf{x} , the output $f(\mathbf{x})$ of our algorithm is computed as:

$$(3.27) \quad f(\mathbf{x}) = \mathcal{N}(\mathbf{x}) + \mathcal{Q}(\mathbf{x}), \quad \text{where } \mathcal{Q}(\mathbf{x}) = \mathcal{Q}_2(\mathbf{x}) + \dots + \mathcal{Q}_{r-1}(\mathbf{x}).$$

3.2.1. $\varepsilon - \delta$ stability and approximate δ -robustness. Note that while manifold regularization allows us to promote $\varepsilon - \delta$ stability for the network \mathcal{N} (final network from [Algorithm 2.1](#)) (see [Corollary 3.11](#)), it is imperative to have a mechanism that promotes $\varepsilon - \delta$ stability for \mathcal{Q} given in [\(3.27\)](#) during the sequential adaptation process. Further, the main motivation of [Algorithm 2.2](#) is to promote robustness. Robustness is the property that if a testing sample is “similar” to a training sample, then the testing error is close to the training error along with the condition that the algorithm fits the training data “well-enough” [[57](#), [24](#)]. If the prediction on the training sample is accurate, then the prediction on a similar testing sample will also be accurate. It is therefore immediately clear that learning a δ -stable function ([Definition 3.6](#)) is necessary for robustness. Additionally, by using a sequence of networks to learn the residuals in [Algorithm 2.2](#), one ensures that the algorithm fits the training data “well-enough”. Since in practice, one fits the training data points to at most ι tolerance (to prevent overfitting), we define approximate δ -robustness as follows:

Definition 3.19 (Approximate δ -robustness). *The function $f(\mathbf{x}) = \mathcal{N}(\mathbf{x}) + \mathcal{Q}(\mathbf{x})$ in [\(3.27\)](#) is called approximately δ -robust at an input $\mathbf{x} \in \mathcal{M}_p^{(0)}$ if each of the networks \mathcal{N} and \mathcal{Q} are δ -stable on $\mathcal{M}_p^{(0)}$ as per [Definition 3.6](#) and $\|f(\mathbf{x}) - c\|_2 \leq \iota$, where c is the correct label for \mathbf{x} and, ι is a small positive constant chosen to prevent overfitting.*

Note that we refrain from the use of any regularizers in [Algorithm 2.2](#) due to the small magnitude of residuals \mathbf{C}_i in [\(3.26\)](#) which inhibits learning in the presence of explicit regularizers. Therefore, one is naturally left with the question on how to design a $\varepsilon - \delta$ stability promoting algorithm for \mathcal{Q} in [Algorithm 2.2](#). [Proposition 3.20](#) provides a practical implicit way of achieving this avoiding the use of any regularizers. *In particular, [proposition 3.20](#) explores how early stopping (a form of implicit regularization in machine learning where a network is trained for a limited number of iterations) can be used to design a $\varepsilon - \delta$ stability promoting algorithm as defined in [Definition 3.4](#). In the below [Proposition 3.20](#), the term “iterations” refer to the number of gradient updates made during the training process.*

Proposition 3.20 ($\varepsilon - \delta$ stability promoting algorithm via early stopping). *Consider the function $\mathcal{Q}(\mathbf{x})$ in [Algorithm 2.2](#) with the input space given in [Definition 3.1](#) and assume that the activation function employed is 1-Lipschitz continuous⁴ for each network \mathcal{Q}_i . Further, assume that the input set $\mathcal{M}_p^{(0)}$ is compact $\forall p$. Then, employing early stopping criteria yields a $\varepsilon - \delta$ stability promoting algorithm for network \mathcal{Q} in [\(3.27\)](#) with $\varepsilon = 0$. That is, there exists a stability function $\delta_p^{\mathcal{Q}}(\zeta) : \left\{ \frac{1}{m^{u+1}}, \frac{1}{m^u}, \dots, 1 \right\} \mapsto \mathbb{R}$ satisfying conditions in [Definition 3.4](#) where $m^u \in \mathbb{Z}^+$ is some chosen upper bound on the training iterations. In particular, $\forall \mathbf{x}, \mathbf{x}' \in \mathcal{M}_p^{(0)} \subset \mathcal{M}^{(0)}$:*

$$(3.28) \quad \|\mathcal{Q}(\mathbf{x}) - \mathcal{Q}(\mathbf{x}')\|_2 \leq \sum_{i=2}^{r-1} \ell^3 \times \left[\prod_{k=1}^3 \left(\sum_{l=0}^{(1/\zeta)-1} \left\| \left(\mathbf{g}_l^{(k)} \right)_i \right\|_2 \right) \right] \times \varepsilon_p = \delta_p^{\mathcal{Q}}(\zeta),$$

where $\varepsilon_p = \sup_{\mathbf{x}, \mathbf{x}' \in \mathcal{M}_p^{(0)}} \|\mathbf{x} - \mathbf{x}'\|_2$, $\left(\mathbf{g}_l^{(k)} \right)_i$ represents the gradients for k^{th} layer weight matrix

⁴We call a function, $h : \mathbb{R}^n \rightarrow \mathbb{R}^m$, 1-Lipschitz continuous if $\forall \mathbf{x}, \mathbf{y} \in \mathbb{R}^n$, $\|h(\mathbf{x}) - h(\mathbf{y})\|_2 \leq \|\mathbf{x} - \mathbf{y}\|_2$.

at the l^{th} iteration of gradient descent for network Q_i ⁵, ℓ denotes a constant learning rate.

Proof. Proof is provided in [Appendix D](#).

Remark 3.21 (Approximate δ -robustness by Algorithm 2.2). Recall [Definition 3.6](#) for δ -stable function. By tuning parameter γ in [\(3.16\)](#), and parameter ζ in [\(3.28\)](#), each network \mathcal{N} and \mathcal{Q} is δ -stable. More information on tuning the parameters for δ -stability are provided in [Appendix E.2](#). Lastly, for an input \mathbf{x} in the training data set, the residual $\|f(\mathbf{x}) - c\|_2 \leq \iota$ in [Definition 3.19](#) is achieved after adding sufficient number of networks leading to approximate δ -robustness.

Remark 3.22 (Manifold regularization vs. early stopping). Note that even though both manifold regularization and early stopping helps one design a ε - δ - stability promoting algorithm, it is important to note the subtle difference between the stability functions $\delta_p^{\mathcal{N}}(\gamma, \xi^{(2)}, \dots, \xi^{(L)})$ in [\(3.16\)](#) and $\delta_p^{\mathcal{Q}}(\zeta)$ in [\(3.28\)](#). While $\delta_p^{\mathcal{N}}(\gamma, \xi^{(2)}, \dots, \xi^{(L)})$ explicitly depends on the geometry (similarity) of data points, the stability function $\delta_p^{\mathcal{Q}}(\zeta)$ is a discrete function that does not directly depend on the geometry of the dataset. In our numerical examples (see results in [subsection 4.1](#)), we demonstrate that the δ -stability enforced by manifold regularization in [Algorithm 2.1](#) is indispensable for achieving better generalization performance in comparison to a baseline trained with a pure early stopping criteria.

4. Numerical Experiments. In this section, we numerically demonstrate the proposed approach on both simulated data sets and real world data sets as follows:

1. Regression task: Boston house price prediction problem.
2. Physics informed adaptive neural network (PIANN).
3. Adaptive learning of inverse maps from sparse data.
4. Image classification problem: MNIST data set.

General experimental settings for all the problems and descriptions of methods adopted for comparison are described in [Appendix E](#). We will show in our numerical experiments that the use of [Algorithm 2.2](#) is inevitable for problems 1 and 4 to deal with the training saturation problem as described in [Corollary 3.16](#). However, the nature of problems 2 and 3 allows us to devise a different hyperparameter settings that evades the use of [Algorithm 2.2](#) (by mitigating the training saturation problem).

4.1. Regression task: Boston house price prediction problem. This regression problem aims to predict the housing prices in Boston and is a common prototype problem for testing ML regression algorithms [9, 19, 46]. The input setting for [Algorithm 2.1](#) and [Algorithm 2.2](#) as well as other details are provided in [Appendix F](#) and [Appendix J](#).

The layerwise training curve is shown in [Figure 2](#) which shows that, subsequent layers are able to learn on top of the representations of previous layers. The percentage of active and inactive parameters (consequence of sparsity regularization) in each layer is shown in [Figure 2](#). From [Figure 2](#) it is clear that initial layers matter more in a deep neural network requiring more number of parameters [41]. We also note from [Figure 2](#) that [Algorithm 2.1](#) is only capable of reducing the training loss to 24.2 and training saturates (negligible decrease in the loss) as predicted in [Corollary 3.16](#).

⁵ $(\mathbf{g}_0^{(k)})_i$ represents the initial weights.

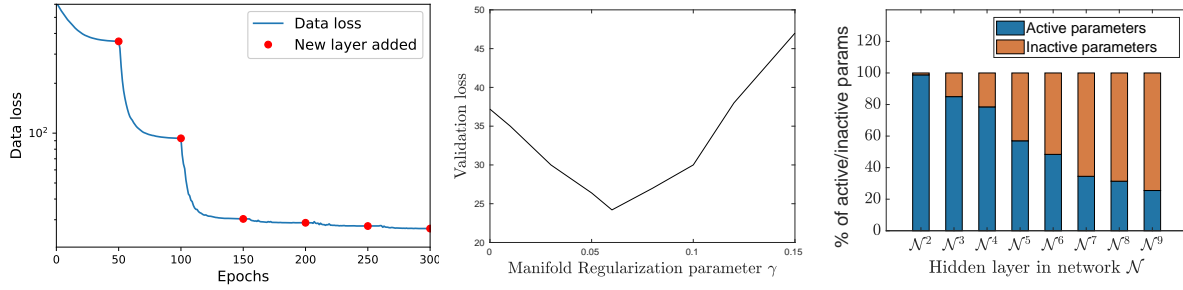
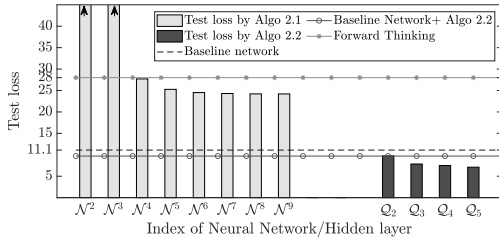


Figure 2. Left to right: layerwise training curve on Boston house price prediction problem by [Algorithm 2.1](#); Importance of manifold regularization (γ) in [Algorithm 2.1](#); Active and inactive parameters in each hidden layer.

Further, [Figure 2](#) (middle figure) shows how to choose the optimal stability parameter (manifold regularization parameter γ) for δ -stability as defined in [Definition 3.6](#). The optimal parameter ($\gamma^* = 0.06$) is the one that gives the lowest validation loss. From [Figure 2](#) (middle figure), it is evident that in the absence of manifold regularization (i.e $\gamma = 0$), stability is not promoted and consequently the final validation loss achieved by [Algorithm 2.1](#) is considerably higher in this case. Note that even though we do not have infinitely many training samples as dictated by [Proposition 3.9](#), the effect of manifold regularization is quite pronounced in this case. In order to further decrease the loss (promote approximate δ -robustness), we resort to [Algorithm 2.2](#). The inputs for [Algorithm 2.2](#) are provided in [Appendix J](#).



Method	Test loss	Params. trained simultaneously	Total params.
Proposed	7.11	11,601	48,474
Baseline	11.2	82,301	82,301
Baseline + Algo. 2.2	10.5	82,301	82,905
Forward-Thinking [22]	28.0	11,601	82,301
Approach [22] + Algo. 2.2	11.5	11,601	82,905

Figure 3. Boston house price prediction problem. Comparison between the proposed approach and other methods. As can be seen, the proposed two-stage approach is the most accurate (by a large margin) with the least number of network parameters.

The adaptation results and performance comparison with other methods (the baseline and the approach from [\[22\]](#)) are summarized in [Figure 3](#). From [Figure 3](#), it is clear that our proposed approach outperformed all the other methods by a good margin. The number of trained parameters in each step of [Algorithm 2.2](#) and from other methods is provided as a [Table](#) in [Figure 3](#). As can be seen, the proposed two-stage approach is the most accurate (by a large margin) with the least number of network parameters. Further, a random architec-

ture search based on the approach in [30] produced a best test loss of 9.28 which was also considerably higher than our approach. It is noteworthy that using [Algorithm 2.2](#) on top of the baseline network trained with early stopping criteria (shown in [Figure 3](#)) did not provide much improvements on the result since the baseline network lacks the δ -stability imposed by the manifold regularization. Similar conclusion is observed when applying [Algorithm 2.2](#) on top of forward-thinking approach [22] (see [Table 3](#)).

4.2. Physics informed adaptive neural network (PIANN). Consider partial differential equation (PDE) of the form:

$$(4.1) \quad \mathcal{G}(\mathbf{x}, \mathbf{y}, a) = 0, \quad \text{in } \Omega,$$

$$(4.2) \quad \mathbf{y} = g \quad \text{in } \partial\Omega,$$

where, $a \in \mathcal{A}$ is the PDE coefficient, \mathcal{A} is the parameter space, $\mathbf{y} \in \mathcal{B}$ is the unknown solution, \mathcal{B} is the solution space and the operator $\mathcal{G} : \mathcal{B} \times \mathcal{A} \rightarrow \mathcal{F}$ is in general a non-linear partial differential operator. Physics informed neural networks (PINNs) [60, 33] aims to solve the PDE (4.1) with the prescribed boundary condition (4.2). A lot of skepticism exists regarding the solution time and accuracy of PINNs in comparison to traditional numerical methods [18]. Nevertheless several attempts have been made to accelerate the training of PINNs [36]. In this section we show how a layerwise training process can lead to faster and more accurate solution in comparison to traditional-PINNs. The key is to adapt the neural network architecture with PINN-type loss terms. If one denotes the discretized equations for (4.1) arising out of a weak form as $\hat{\mathcal{G}}^i(y(\mathbf{x}_1), y(\mathbf{x}_2), \dots, y(\mathbf{x}_n))$, $i = 1, \dots, n$, the physics loss function is defined as:

$$(4.3) \quad \Phi_p(\boldsymbol{\theta}) = \sum_{i=1}^n \left[\hat{\mathcal{G}}^i(y(\boldsymbol{\theta}, \mathbf{x}_1), y(\boldsymbol{\theta}, \mathbf{x}_2), \dots, y(\boldsymbol{\theta}, \mathbf{x}_n)) \right]^2,$$

where, $\{\mathbf{x}_1 \dots \mathbf{x}_n\}$ is the set of collocation points in Ω . Further, the neural network learns the boundary condition (4.2) by considering training data points on $\partial\Omega$. It may be noted that, if one requires to update the network for a new parameter field $a \in \mathcal{A}$ or a modified operator \mathcal{G} , it is often unclear on the best layers to re-train [49]. Recent work by Subel et al. [49] shows that common wisdom guided transfer learning in machine learning literature that involves retraining only the last few layers of the network is often not the best option and that interpretable hidden layers are necessary to devise meaningful transfer learning strategy. Our approach (PIANN), attempts to create interpretable hidden layers in a deep network with superior performance compared to traditional PINNs.

For the present approach, $\gamma = 0$ (manifold regularization) since collocation points are uniformly distributed over the domain and the input data clusters does not exist. The training data set contains 4000 data points on the boundary. Further, $n = 961$.

Inspired from the continuation method in optimization [47], we propose the layerwise continuation approach where each layer is tasked with learning a simple function that can be minimized efficiently, and gradually transform it to more complicated cost function upon adding new layers. For achieving this, we choose $\tau^{(i+1)} > \tau^{(i)}$ (τ is the weight on the physics loss), and thereby also ensuring that a newly added layer is trainable ([Proposition 3.15](#)).

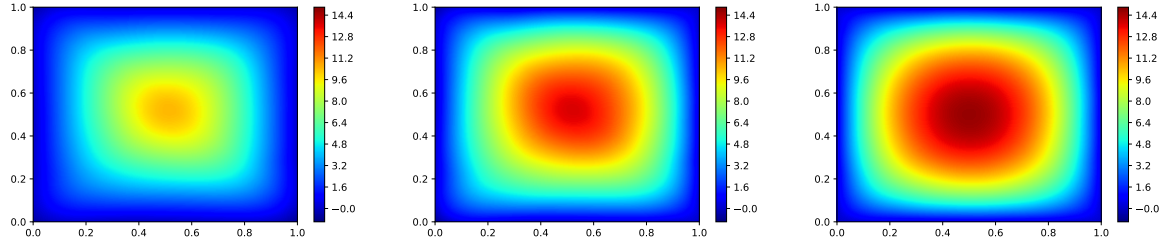


Figure 4. Adaptively learning the Poisson's equation (Case a: symmetric boundary condition). Left to right: Solution after training layer $\mathcal{N}^{(2)}$; Solution after training layer $\mathcal{N}^{(3)}$; Solution after training layer $\mathcal{N}^{(7)}$.

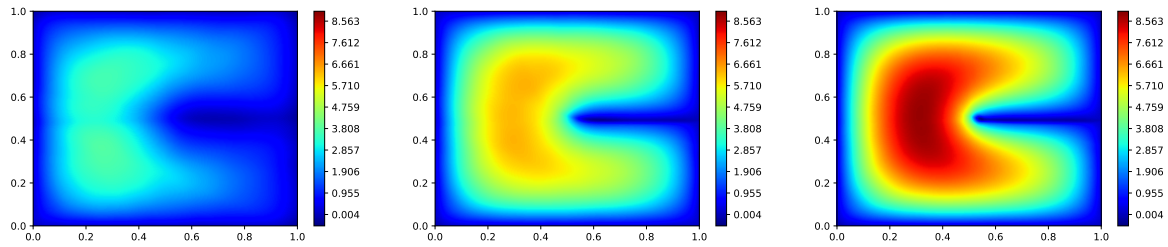


Figure 5. Adaptively learning the Poisson's equation (Case b: Slit in domain). Left to right: solutions after $\mathcal{N}^{(2)}$ layers, $\mathcal{N}^{(3)}$ layers, and $\mathcal{N}^{(5)}$ layers.

Also, since $|\tau^{(i+1)} - \tau^{(i)}| \neq 0$ for any i , training saturation problem does not exist in this case (Corollary 3.16) and Algorithm 2.2 is not required. For demonstration of our approach, we consider prototype problems considered by Weinan et al. [60].

4.2.1. Learning the Poisson equation. For demonstration, we consider solving the Poisson equation where the operator $\mathcal{G}(\mathbf{x}, \mathbf{y}, a)$ in (4.1) is given as:

$$(4.4) \quad \mathcal{G}(\mathbf{x}, \mathbf{y}, a) = -\nabla \cdot (a(x_1, x_2) \nabla y) - f(x_1, x_2) \quad \text{in } \Omega \subset \mathbb{R}^2,$$

$$(4.5) \quad y = 0 \quad \text{in } \partial\Omega,$$

with $a(x_1, x_2) = 1$ and $f(x_1, x_2) = 200$. Further, we experiments are conducted for two different domains:

1. Case (a): $\Omega = (0, 1) \times (0, 1)$;
2. Case (b): $\Omega = (0, 1) \times (0, 1) - (0.5, 1) \times \{0.5\}$ [59]

Additional details on training process are given in Appendix G. The evolution of PDE solution $y(\mathbf{x})$ as more layers are added is shown in Figure 4 and 5: with 5 layers the solution looks identical to the finite element solution. Note that learning the solution progressively by our proposed approach (trained for a total of 8000 epochs) outperformed a baseline (traditional PINNs trained for 15000 epochs) trained under similar settings as seen from Figure 6. It can be seen that layerwise training procedure by Hettinger et al. [22] performed poorly in this case since by this method the network output is not preserved after adding a new layer. The

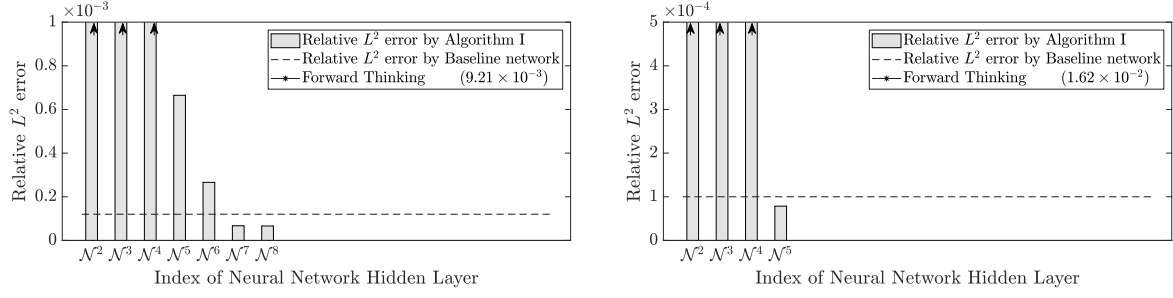


Figure 6. PIANN problem. Comparison of the proposed approach and others. Case a: Symmetric boundary condition (left figure), Case b: Slit in domain (right figure).

summary of results and parameter efficiency is provided in [Appendix G](#). Further, creating interpretable hidden layers in a deep network helps one in devising efficient transfer learning strategies and make informed decisions on which layers to re-train. An example is provided in [Appendix H](#) where we demonstrate the superiority of our approach over traditional transfer learning strategies.

4.3. Adaptive learning of inverse maps from sparse data. Inverse problems are usually ill-posed and involves learning a map from low-dimensional space (observation space) to a high dimensional space (parameter space). This pose a challenge for learning the inverse map especially in the low data regime. Further, it is desirable for the inverse map to be well-posed where the solution's behaviour should change continuously with respect to input. Therefore, it is clear that the notion of δ -stability defined in [Definition 3.2](#) is closely related to the concept of well-posedness. Therefore, the developed procedure serves as a natural candidate for this problem and we show how our approach can be applied to this regression task characterized by low availability of data. In this section, we demonstrate the approach for conductivity coefficient field inversion in a 2D heat equation written as:

$$(4.6) \quad \begin{aligned} -\nabla \cdot (e^u \nabla y) &= 20 & \text{in } \Omega = [0, 1]^2, \\ y &= 0 & \text{on } \Gamma^{\text{ext}}, \\ \mathbf{n} \cdot (e^u \nabla y) &= 0 & \text{on } \Gamma^{\text{root}}, \end{aligned}$$

where \mathbf{n} is normal vector on the equivalent boundary surfaces. The parameter of interest is denoted as u and the observables are 10 pointwise values of the heat state (measurement locations are shown in [Figure 8](#)), \mathbf{y} at arbitrary location. The training data is generated by drawing parameter samples as:

$$(4.7) \quad \mathbf{u}(\mathbf{x}) = \sum_{i=1}^n \sqrt{\lambda_i} \phi_i x_i$$

where λ_i , ϕ_i is the eigen-pair of an exponential two point correlation function and $\mathbf{x} = (x_1, \dots, x_n)$ is drawn from standard Gaussian distribution [[13](#)]. Note that \mathbf{x} represents the output of the network. For the present study, we choose the output dimension $n = 12$. The

Table 1
Relative error achieved by baseline network and other methods

Training data size	Equivalent baseline	Proposed method	Forward thinking [22]	Architecture search (AS) [30]
20	0.64	0.585	1.41	0.625
50	0.44	0.42	0.84	0.427

observation vector (input of the network) is generated by solving (4.6). 5% additive Gaussian noise is added to the observations to represent field condition.

We consider experiments with two different training data size; 20 and 50. The validation data set consists of 20 data points and the test set contains 500 data points. Since the number of training data points is too low, forming clusters with the available dataset is impractical.

4.3.1. Forming artificial data clusters and training procedure. In order to compute the manifold regularization (2.4), we generate artificial clusters by first assuming that each input data point (observation) lies on a different cluster, i.e $\mathbf{x}_m \in \mathcal{M}_m \subset \mathbb{R}^{10}$. Each set \mathcal{M}_m is then populated with 100 artificial perturbations of the input \mathbf{x}_m (assuming 1% additive Gaussian noise) and we further assume that each perturbed data is a valid observation data point.

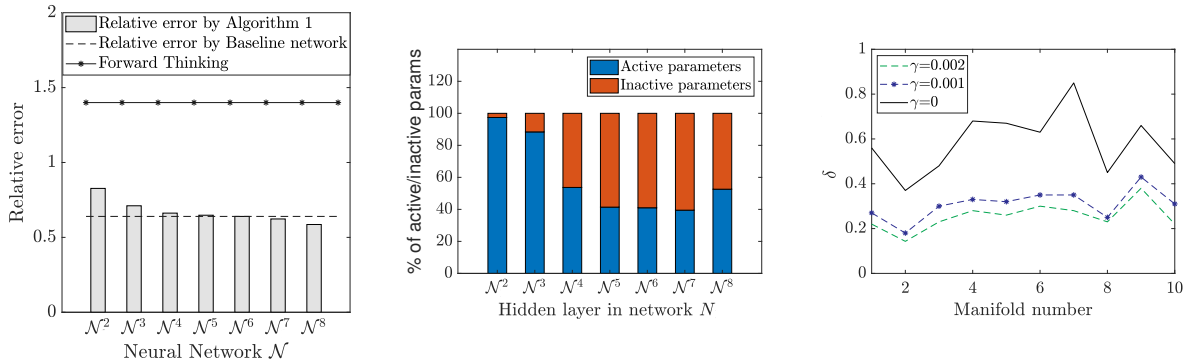


Figure 7. Summary of adaptive inversion (trained with 20 data set). Left to right: Summary of Algorithm 2.1; Active and inactive parameters in each hidden layer; Promoting δ -stability through manifold regularization.

In addition, we consider increasing the manifold regularization weight, $\gamma^{(i+1)} = 2 \times \gamma^{(i)}$ while adding new layers where stability is more strongly enforced in the later layers. This strategy is adopted due to the small data-set size of the problem where initial layers are weakly regularized to allow for maximum information transfer through the initial layers (note that we freeze the parameters of these layers later). Further, for this problem setup we have numerically observed that the data loss Φ_d in (2.6) only increases marginally while optimizing the later layers (where $\gamma^{(i)}$ is too large) making this strategy feasible. Most importantly, note that by Proposition 3.15, training does not saturate since $\gamma^{(i+1)} = 2 \times \gamma^{(i)}$ (satisfying the necessary condition for trainability) and hence one does not require Algorithm 2.2.

The relative error achieved by different methods is shown in Table 1 and Figure 7 which

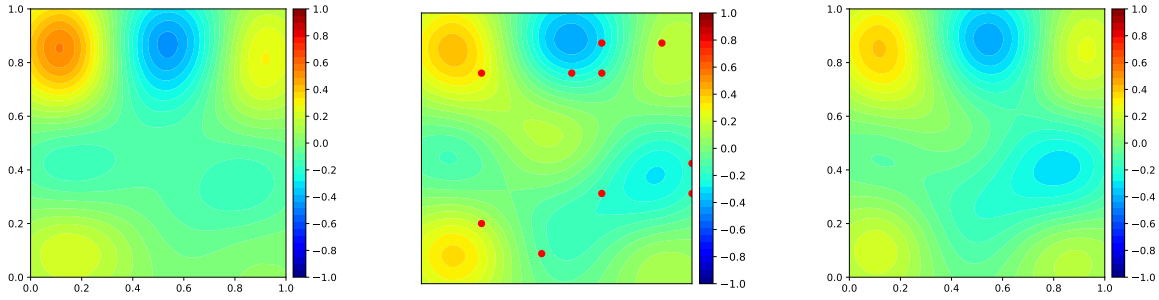


Figure 8. Predicted parameter field for a particular test observation sample using different methods (trained with 50 data sets). First row left to right: Solution obtained by baseline network; Exact solution (red dot shows the location of sensors measuring the heat state); Solution obtained by Algorithm 2.1.

clearly shows that Algorithm 2.1 outperforms traditional methods. Further, Figure 8 also shows that the parameter field predicted by the proposed method is better than the one produced by baseline network.

Since for this problem, data can be artificially generated from each \mathcal{M}_m , one could investigate the effect of manifold regularization numerically through on a sampling based approach. We study the nature of the stability function $\delta_j^{\mathcal{N}}(\gamma)$ in (3.16) by training three networks exactly in the same way but with different $\gamma^{(2)}$. Once the network is trained, 5000 different points $\{\mathbf{x}_1, \dots, \mathbf{x}_{5000}\} \in \mathcal{M}_m$ is artificially generated. Then, based on (3.16), an upper bound corresponding to the set \mathcal{M}_m is approximately computed as:

$$(4.8) \quad \delta_m^{\mathcal{N}}(\gamma^{(2)}) = \max_{i,j} \left(\|\mathcal{N}(\mathbf{x}_j) - \mathcal{N}(\mathbf{x}_i)\|_2 \right), \quad \mathbf{x}_i, \mathbf{x}_j \in \mathcal{M}_m$$

Figure 7 shows that as γ is increased, the numerically computed $\delta_m^{\mathcal{N}}(\gamma^{(2)})$ decreases almost surely $\forall m$ and provides a feasible way for controlling stability via manifold regularization. In addition, the evolution of solution across the hidden layers for a particular test observation sample is shown in Figure 9. It is clear from Figure 9 that injecting stability in later layers allows the network to recover fine details in the parameter field when the baseline network fails to do so.

4.4. Image classification problem: MNIST data set. Finally, we consider the MNIST handwritten digit classification problem using a fully connected residual neural network. It is noteworthy that, even though MNIST problem is easier to solve with convolutional architectures, achieving high classification accuracy remains challenging with fully connected networks. In this section we examine how the design of $\varepsilon - \delta$ stability promoting algorithm allows us to achieve a high accuracy using fully-connected networks. We demonstrate the adaptation procedure for two different scenarios: a) Case with 20 neurons in each hidden layer; b) Case with 500 neurons in each hidden layer. Figure 10 shows that the proposed methodology outperforms the baseline network and other methods by noticeable margins and even exhibiting performance on par to that of a LeNet-5 architecture (a basic CNN architecture). Further, Figure 11 shows the schematic of Algorithm 2.1 applied to the MNIST dataset. Note that the inactive parameters can be removed after training each hidden layer

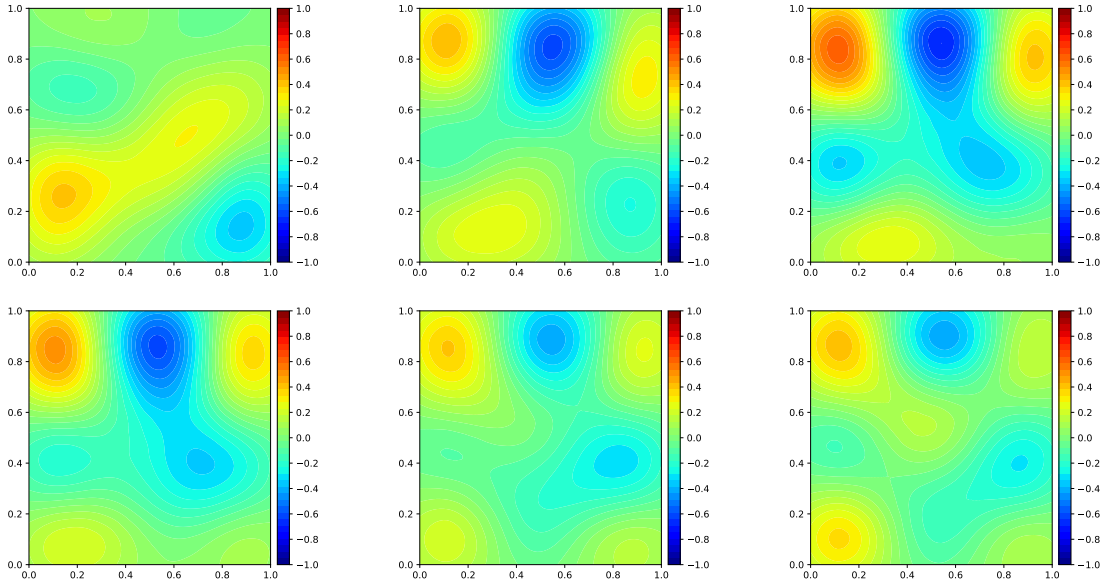


Figure 9. Evolution of parameter field across the hidden layers for a particular test observation sample. First row left to right: Solution after training layer $N^{(3)}$; Solution after training layer $N^{(5)}$; Solution after training layer $N^{(7)}$. Second row left to right: Solution after training layer $N^{(9)}$; Solution after training layer $N^{(12)}$; Exact solution.

as demonstrated in Figure 11 thereby leading to a partially connected network. Additional details on experiments carried out is provided in Appendix I.

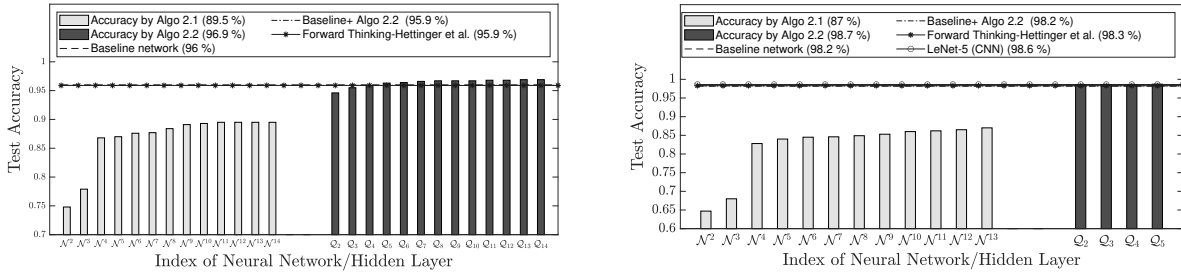


Figure 10. MNIST classification problem. Left figure is with 20 neurons in each hidden layer: our approach provides the best results with 96.9% testing accuracy. Right figure is with 500 neurons in each hidden layer: our approach provides the best results with 98.7% testing accuracy.

5. Concluding remarks. In this paper, we presented a two-stage procedure for adaptive learning that promotes “robustness” and thereby generalizing well for a given data-set. The first stage (Algorithm 2.1) is designed to grow a neural network along the depth while promoting δ -stability for each hidden layer through the use of manifold regularization. In addition, non-important parameters are removed using a sparsity promoting regularization. We have proved that for certain hyperparameter settings of Algorithm 2.1, one faces with the training

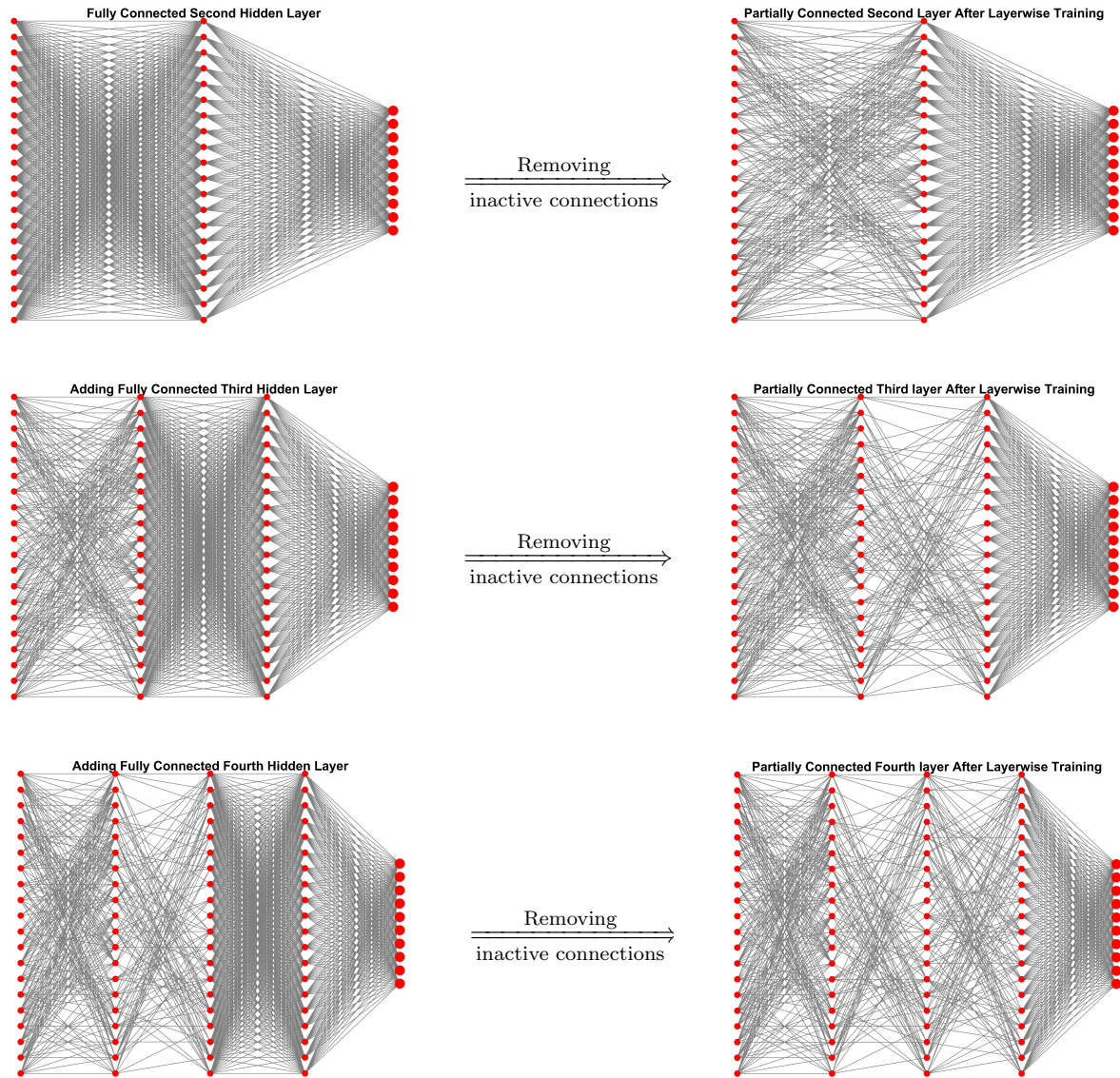


Figure 11. Schematic of *Algorithm 2.1* demonstrated on MNIST dataset (20 neurons in each hidden layer) for the first few layers: Note that the input layer and ResNet connections are not shown here.

saturation problem where the newly added layer does not learn ([Corollary 3.16](#)). In order to further improve the prediction accuracy, we designed [Algorithm 2.2](#) as a post-processing stage where the main goal is to promote robustness ([Definition 3.19](#)). Besides several theoretical results, numerical results on prototype regression and classification tasks, including solving forward and inverse problems governed by elliptic PDEs, suggest that the proposed approach can outperform an ad-hoc baseline and other adaptation strategies in terms of generalization error. The proposed PIANN is perhaps the first PINN approaches that is capable of adapting

the network architecture with theoretical results on stabilities.

Acknowledgement. This research is partially funded by the National Science Foundation awards NSF-OAC-2212442, NSF-2108320, and NSF-CAREER-1845799; and by the Department of Energy award DE-SC0018147 and DE-SC0022211. The authors would also like to thank Dr. Hwan Goh, Dr. Jonathan Wittmer, Hai Van Nguyen, and Jau-Wei Chen for fruitful discussions. The authors also acknowledge the Texas Advanced Computing Center (TACC) at The University of Texas at Austin for providing HPC, visualization, database, or grid resources that have contributed to some of the results reported within this paper. URL: <http://www.tacc.utexas.edu>.

REFERENCES

- [1] P. BALAPRAKASH, M. SALIM, T. D. URAM, V. VISHWANATH, AND S. M. WILD, *Deephyper: Asynchronous hyperparameter search for deep neural networks*, in 2018 IEEE 25th international conference on high performance computing (HiPC), IEEE, 2018, pp. 42–51.
- [2] E. BELILOVSKY, M. EICKENBERG, AND E. OYALLON, *Greedy layerwise learning can scale to imagenet*, in International conference on machine learning, PMLR, 2019, pp. 583–593.
- [3] M. BELKIN AND P. NIYOGI, *Towards a theoretical foundation for laplacian-based manifold methods*, Journal of Computer and System Sciences, 74 (2008), pp. 1289–1308.
- [4] M. BELKIN, P. NIYOGI, AND V. SINDHWANI, *Manifold regularization: A geometric framework for learning from labeled and unlabeled examples.*, Journal of machine learning research, 7 (2006).
- [5] Y. BENGIO, P. LAMBLIN, D. POPOVICI, H. LAROCHELLE, ET AL., *Greedy layer-wise training of deep networks*, Advances in neural information processing systems, 19 (2007), p. 153.
- [6] S. BUBECK, Y. LI, AND D. M. NAGARAJ, *A law of robustness for two-layers neural networks*, in Conference on Learning Theory, PMLR, 2021, pp. 804–820.
- [7] S. BUBECK AND M. SELLKE, *A universal law of robustness via isoperimetry*, Advances in Neural Information Processing Systems, 34 (2021), pp. 28811–28822.
- [8] D. CHARALAMBOS AND B. ALIPRANTIS, *Infinite Dimensional Analysis: A Hitchhiker’s Guide*, Springer-Verlag Berlin and Heidelberg GmbH & Company KG, 2013.
- [9] S. CHATTERJEE, A. M. JAVID, M. SADEGHI, P. P. MITRA, AND M. SKOGLUND, *Progressive learning for systematic design of large neural networks*, arXiv preprint arXiv:1710.08177, (2017).
- [10] T. CHEN, I. GOODFELLOW, AND J. SHLENS, *Net2net: Accelerating learning via knowledge transfer*, arXiv preprint arXiv:1511.05641, (2015).
- [11] B. A. CLEGG, G. J. DIGIROLAMO, AND S. W. KEELE, *Sequence learning*, Trends in cognitive sciences, 2 (1998), pp. 275–281.
- [12] D.-A. CLEVERT, T. UNTERTHINER, AND S. HOCHREITER, *Fast and accurate deep network learning by exponential linear units (elus)*, arXiv preprint arXiv:1511.07289, (2015).
- [13] P. G. CONSTANTINE, C. KENT, AND T. BUI-THANH, *Accelerating markov chain monte carlo with active subspaces*, SIAM Journal on Scientific Computing, 38 (2016), pp. A2779–A2805.
- [14] M. P. DO CARMO AND J. FLAHERTY FRANCIS, *Riemannian geometry*, vol. 6, Springer, 1992.
- [15] D. ELLIS AND N. MORGAN, *Size matters: An empirical study of neural network training for large vocabulary continuous speech recognition*, in 1999 IEEE International Conference on Acoustics, Speech, and Signal Processing. Proceedings. ICASSP99 (Cat. No. 99CH36258), vol. 2, IEEE, 1999, pp. 1013–1016.
- [16] T. ELSKEN, J. H. METZEN, AND F. HUTTER, *Efficient multi-objective neural architecture search via lamarckian evolution*, arXiv preprint arXiv:1804.09081, (2018).
- [17] C. FEFFERMAN, S. MITTER, AND H. NARAYANAN, *Testing the manifold hypothesis*, Journal of the American Mathematical Society, 29 (2016), pp. 983–1049.
- [18] T. G. GROSSMANN, U. J. KOMOROWSKA, J. LATZ, AND C.-B. SCHÖNLIEB, *Can physics-informed neural networks beat the finite element method?*, IMA Journal of Applied Mathematics, (2024), p. hxae011.
- [19] D. HARRISON JR AND D. L. RUBINFELD, *Hedonic housing prices and the demand for clean air*, Journal

- of environmental economics and management, 5 (1978), pp. 81–102.
- [20] K. HE, X. ZHANG, S. REN, AND J. SUN, *Deep residual learning for image recognition*, in Proceedings of the IEEE conference on computer vision and pattern recognition, 2016, pp. 770–778.
- [21] K. HE, X. ZHANG, S. REN, AND J. SUN, *Identity mappings in deep residual networks*, in European conference on computer vision, Springer, 2016, pp. 630–645.
- [22] C. HETTINGER, T. CHRISTENSEN, B. EHLERT, J. HUMPHERYS, T. JARVIS, AND S. WADE, *Forward thinking: Building and training neural networks one layer at a time*, arXiv preprint arXiv:1706.02480, (2017).
- [23] G. E. HINTON, *Learning multiple layers of representation*, Trends in cognitive sciences, 11 (2007), pp. 428–434.
- [24] C. JIN AND M. RINARD, *Manifold regularization for locally stable deep neural networks*, arXiv preprint arXiv:2003.04286, (2020).
- [25] D. P. KINGMA AND J. BA, *Adam: A method for stochastic optimization*, arXiv preprint arXiv:1412.6980, (2014).
- [26] M. KULKARNI AND S. KARANDE, *Layer-wise training of deep networks using kernel similarity*, arXiv preprint arXiv:1703.07115, (2017).
- [27] Y. LECUN, Y. BENGIO, ET AL., *Convolutional networks for images, speech, and time series*, The handbook of brain theory and neural networks, 3361 (1995), p. 1995.
- [28] T. LEE, M. CHOI, AND S. YOON, *Manifold regularized deep neural networks using adversarial examples*, arXiv preprint arXiv:1511.06381, (2015).
- [29] R. LENGELLÉ AND T. DENOËUX, *Training mlps layer by layer using an objective function for internal representations*, Neural Networks, 9 (1996), pp. 83–97.
- [30] L. LI AND A. TALWALKAR, *Random search and reproducibility for neural architecture search*, in Uncertainty in artificial intelligence, PMLR, 2020, pp. 367–377.
- [31] Y. LIU, Y. SUN, B. XUE, M. ZHANG, G. G. YEN, AND K. C. TAN, *A survey on evolutionary neural architecture search*, IEEE transactions on neural networks and learning systems, (2021).
- [32] C.-Y. LOW, J. PARK, AND A. B.-J. TEOH, *Stacking-based deep neural network: deep analytic network for pattern classification*, IEEE transactions on cybernetics, 50 (2019), pp. 5021–5034.
- [33] L. LU, X. MENG, Z. MAO, AND G. E. KARNIADAKIS, *Deepxde: A deep learning library for solving differential equations*, SIAM review, 63 (2021), pp. 208–228.
- [34] X. MA AND W. LIU, *Recent advances of manifold regularization*, Manifolds II-Theory and Applications, (2018).
- [35] J. MACQUEEN ET AL., *Some methods for classification and analysis of multivariate observations*, in Proceedings of the fifth Berkeley symposium on mathematical statistics and probability, vol. 1, Oakland, CA, USA, 1967, pp. 281–297.
- [36] S. MARKIDIS, *The old and the new: Can physics-informed deep-learning replace traditional linear solvers?*, Frontiers in big Data, (2021), p. 92.
- [37] R. MIKKULAINEN, J. LIANG, E. MEYERSON, A. RAWAL, D. FINK, O. FRANCON, B. RAJU, H. SHAHRZAD, A. NAVRUZAN, N. DUFFY, ET AL., *Evolving deep neural networks*, in Artificial intelligence in the age of neural networks and brain computing, Elsevier, 2019, pp. 293–312.
- [38] G. MONTAVON, K.-R. MÜLLER, AND M. BRAUN, *Layer-wise analysis of deep networks with gaussian kernels*, Advances in neural information processing systems, 23 (2010), pp. 1678–1686.
- [39] H.-T. NGUYEN, C. C. CHEAH, AND K.-A. TOH, *An analytic layer-wise deep learning framework with applications to robotics*, arXiv preprint arXiv:2102.03705, (2021).
- [40] J. T. ODEN AND L. DEMKOWICZ, *Applied functional analysis*, Chapman and Hall/CRC, 2017.
- [41] M. RAGHU, B. POOLE, J. KLEINBERG, S. GANGULI, AND J. SOHL-DICKSTEIN, *On the expressive power of deep neural networks*, in international conference on machine learning, PMLR, 2017, pp. 2847–2854.
- [42] M. RAISSI, P. PERDIKARIS, AND G. E. KARNIADAKIS, *Physics-informed neural networks: A deep learning framework for solving forward and inverse problems involving nonlinear partial differential equations*, Journal of Computational Physics, 378 (2019), pp. 686–707.
- [43] E. REAL, A. AGGARWAL, Y. HUANG, AND Q. V. LE, *Regularized evolution for image classifier architecture search*, in Proceedings of the aaai conference on artificial intelligence, vol. 33, 2019, pp. 4780–4789.
- [44] D. RUEDA-PLATA, R. RAMOS-POLLÁN, AND F. A. GONZÁLEZ, *Supervised greedy layer-wise training for deep convolutional networks with small datasets*, in Computational Collective Intelligence, Springer,

- 2015, pp. 275–284.
- [45] M. D. SAMAD AND A. SEKMEN, *Manifold regularized convolutional neural network*, in 2021 International Conference on Engineering and Emerging Technologies (ICEET), IEEE, 2021, pp. 1–6.
- [46] M. SHAHHOSSEINI, G. HU, AND H. PHAM, *Optimizing ensemble weights for machine learning models: A case study for housing price prediction*, in INFORMS International Conference on Service Science, Springer, 2019, pp. 87–97.
- [47] A. SHAMELI AND Y. ABBASI-YADKORI, *A continuation method for discrete optimization and its application to nearest neighbor classification*, arXiv preprint arXiv:1802.03482, (2018).
- [48] K. O. STANLEY AND R. MIIKKULAINEN, *Evolving neural networks through augmenting topologies*, Evolutionary computation, 10 (2002), pp. 99–127.
- [49] A. SUBEL, Y. GUAN, A. CHATTOPADHYAY, AND P. HASSANZADEH, *Explaining the physics of transfer learning a data-driven subgrid-scale closure to a different turbulent flow*, arXiv preprint arXiv:2206.03198, (2022).
- [50] M. SUGANUMA, S. SHIRAKAWA, AND T. NAGAO, *A genetic programming approach to designing convolutional neural network architectures*, in Proceedings of the genetic and evolutionary computation conference, 2017, pp. 497–504.
- [51] L. Q. TRINH, *Greedy layerwise training of convolutional neural networks*, PhD thesis, Massachusetts Institute of Technology, 2019.
- [52] R. VERSHYNIN, *High-dimensional probability: An introduction with applications in data science*, vol. 47, Cambridge university press, 2018.
- [53] L. WU, D. WANG, AND Q. LIU, *Splitting steepest descent for growing neural architectures*, Advances in Neural Information Processing Systems, 32 (2019).
- [54] M. WYNNE-JONES, *Node splitting: A constructive algorithm for feed-forward neural networks*, Neural Computing & Applications, 1 (1993), pp. 17–22.
- [55] X. XIAO, T. B. MUDIYANSELAGE, C. JI, J. HU, AND Y. PAN, *Fast deep learning training through intelligently freezing layers*, in 2019 International Conference on Internet of Things (iThings) and IEEE Green Computing and Communications (GreenCom) and IEEE Cyber, Physical and Social Computing (CPSCom) and IEEE Smart Data (SmartData), IEEE, 2019, pp. 1225–1232.
- [56] D. XU AND J. C. PRINCIPE, *Training mlps layer-by-layer with the information potential*, in IJCNN'99. International Joint Conference on Neural Networks. Proceedings (Cat. No. 99CH36339), vol. 3, IEEE, 1999, pp. 1716–1720.
- [57] H. XU AND S. MANNOR, *Robustness and generalization*, Machine learning, 86 (2012), pp. 391–423.
- [58] Y.-Y. YANG, C. RASHTCHIAN, H. ZHANG, R. R. SALAKHUTDINOV, AND K. CHAUDHURI, *A closer look at accuracy vs. robustness*, Advances in neural information processing systems, 33 (2020), pp. 8588–8601.
- [59] B. YU ET AL., *The deep ritz method: a deep learning-based numerical algorithm for solving variational problems*, arXiv preprint arXiv:1710.00211, (2017).
- [60] B. YU ET AL., *The deep ritz method: a deep learning-based numerical algorithm for solving variational problems*, Communications in Mathematics and Statistics, 6 (2018), pp. 1–12.
- [61] B. ZOPH AND Q. V. LE, *Neural architecture search with reinforcement learning*, arXiv preprint arXiv:1611.01578, (2016).

Appendix A. Proof of non-asymptotic bound in equation (3.8). Let us first define the random variable X_i as follows:

$$(A.1) \quad \begin{aligned} X_i &= \int_{\mathcal{M}_p^{(1)}} \left\| \mathcal{N}^{(2)}(\mathbf{x}_i) - \mathcal{N}^{(2)}(\mathbf{y}) \right\|_2^2 d\mu_p^{(1)}(\mathbf{y}), \quad \mathbf{x}_i \sim \mu_p^{(1)}(\mathbf{x}), \\ \mathbb{E}[X_i] &= \int_{\mathcal{M}_p^{(1)}} \int_{\mathcal{M}_p^{(1)}} \left\| \mathcal{N}^{(2)}(\mathbf{x}) - \mathcal{N}^{(2)}(\mathbf{y}) \right\|_2^2 d\mu_p^{(1)}(\mathbf{x}) d\mu_p^{(1)}(\mathbf{y}). \end{aligned}$$

Now using assumption 1 (continuous function $\mathcal{N}^{(1)}$ maps the compact set $\mathcal{M}_p^{(0)}$ to $\mathcal{M}_p^{(1)}$ which is compact) it is easy to see that X_i is a bounded random variable based on the Weierstrass

theorem (Theorem 1.18.1 in [40]). Therefore, from Hoeffding's inequality [52] we have:

$$\mathbb{P} \left(\left| \frac{1}{m_p} \sum_{i=1}^{m_p} X_i - \mathbb{E}[X_i] \right| \geq \varepsilon \right) \leq 2 \exp(-2c_1 m_p \varepsilon^2),$$

where c_1 is a positive constant. Thus,

$$(A.2) \quad \mathbb{P} \left(\mathbb{E}[X_i] \leq \varepsilon + \frac{1}{m_p} \sum_{i=1}^{m_p} X_i \right) \geq \mathbb{P} \left(\left| \frac{1}{m_p} \sum_{i=1}^{m_p} X_i - \mathbb{E}[X_i] \right| < \varepsilon \right) \geq 1 - 2 \exp(-2c_1 m_p \varepsilon^2),$$

Now for any given $\mathbf{x}_i \in \mathcal{M}_p^{(1)}$ drawn from $\mu_p^{(1)}(\mathbf{x})$, let us define the following random variable:

$$(A.3) \quad \begin{aligned} Y_j^i &= \left\| \mathcal{N}^{(2)}(\mathbf{x}_i) - \mathcal{N}^{(2)}(\mathbf{y}_j) \right\|_2^2, \quad \mathbf{y}_j \sim \mu_p^{(1)}(\mathbf{y}), \\ \mathbb{E}[Y_j^i] &= \int_{\mathcal{M}_p^{(1)}} \left\| \mathcal{N}^{(2)}(\mathbf{x}_i) - \mathcal{N}^{(2)}(\mathbf{y}) \right\|_2^2 d\mu_p^{(1)}(\mathbf{y}). \end{aligned}$$

Again, from Hoeffding's inequality for random variable Y_j^i we have:

$$\mathbb{P} \left(\left| \frac{1}{m_p} \sum_{j=1}^{m_p} Y_j^i - \mathbb{E}[Y_j^i] \right| \geq \varepsilon \right) \leq 2 \exp(-2c_2 m_p \varepsilon^2),$$

where c_2 is a positive constant. Therefore, we have:

$$(A.4) \quad \mathbb{P} \left(\mathbb{E}[Y_j^i] \leq \varepsilon + \frac{1}{m_p} \sum_{j=1}^{m_p} Y_j^i \right) \geq \mathbb{P} \left(\left| \frac{1}{m_p} \sum_{j=1}^{m_p} Y_j^i - \mathbb{E}[Y_j^i] \right| \leq \varepsilon \right) \geq 1 - 2 \exp(-2c_2 m_p \varepsilon^2).$$

Now considering the concentration inequality (A.4) for all i (summing up), and using the union bound we have:

$$(A.5) \quad \mathbb{P} \left(\frac{1}{m_p} \sum_{i=1}^{m_p} \mathbb{E}[Y_j^i] \leq \varepsilon + \frac{1}{m_p^2} \sum_{i=1}^{m_p} \sum_{j=1}^{m_p} Y_j^i \right) \geq 1 - 2m_p \exp(-2c_2 m_p \varepsilon^2).$$

Now combining the result (A.2) and (A.5) and using the union bound, we have:

$$\mathbb{P} \left(\mathbb{E}[X_i] \leq \varepsilon + \frac{1}{m_p^2} \sum_{i=1}^{m_p} \sum_{j=1}^{m_p} Y_j^i \right) \geq 1 - 2m_p \exp(-c_3 m_p \varepsilon^2) - 2 \exp(-c_4 m_p \varepsilon^2) = 1 - \mathcal{E}_p^{(2)}(m_p, \varepsilon)$$

where, the constants c_3, c_4 depends on the cluster C_p and the hidden layer. Therefore, we have the final required result:

$$\mathbb{P} \left[\mathbb{E}_{\mu_p^{(1)}} \left[\left\| \mathcal{N}^{(2)}(\mathbf{x}) - \mathcal{N}^{(2)}(\mathbf{y}) \right\|_2^2 \right] \leq \varepsilon + \frac{1}{m_p^2} \sum_{\mathbf{x}_i, \mathbf{x}_j \in C_p} \left\| \mathcal{N}^{(2)}(\mathbf{x}_i) - \mathcal{N}^{(2)}(\mathbf{x}_j) \right\|_2^2 \right] \geq 1 - \mathcal{E}_p^{(2)}(m_p, \varepsilon).$$

Appendix B. Proof of Corollary 3.11. A sketch of the proof is provided here. Since \mathcal{N} is a composition of hidden layers (note that $(L+1)^{th}$ layer is the output layer), we have:

$$\mathcal{N}(\mathbf{x}) = \mathcal{N}^{(L+1)} \circ \mathcal{R}^{(L)} \circ \mathcal{N}^{(L)} \circ \dots \circ \mathcal{R}^{(1)} \circ \mathcal{N}^{(1)}(\mathbf{x}).$$

Since the activation function employed is Lipschitz continuous, we have $\forall \mathbf{x}, \mathbf{x}' \in \mathcal{M}_p^{(L-1)}$:

$$(B.1) \quad \left\| \mathcal{N}^{(L)}(\mathbf{x}) - \mathcal{N}^{(L)}(\mathbf{x}') \right\|_2^2 \leq c^{(L)} \times \|\mathbf{x} - \mathbf{x}'\|_2^2,$$

$$(B.2) \quad \left\| \mathcal{N}^{(L)}(\mathbf{x}) - \mathcal{N}^{(L)}(\mathbf{x}') \right\|_2^2 \leq \tilde{\delta}_p \left(\kappa^{L-2} \times \gamma, \xi^{(L)} \right),$$

where $c^{(L)} \geq 0$, and (B.2) holds with probability at-least $\left(1 - \xi^{(L)} - \mathcal{E}_p^{(L)}(m_p, \xi^{(L)}\varepsilon)\right)$ (from (3.6)). Now multiplying (B.1) and (B.2), we have:

$$(B.3) \quad \begin{aligned} & \left\| \mathcal{N}^{(L)}(\mathbf{x}) - \mathcal{N}^{(L)}(\mathbf{x}') \right\|_2^2 \leq \\ & \sqrt{c^{(L)}} \times \sqrt{\tilde{\delta}_p \left(\kappa^{L-2} \times \gamma, \xi^{(L)} \right)} \times \left\| \mathcal{R}^{(L-1)} \left(\mathcal{N}^{(L-1)}(\mathbf{y}) \right) - \mathcal{R}^{(L-1)} \left(\mathcal{N}^{(L-1)}(\mathbf{y}') \right) \right\|_2 \\ & \leq c^{(L)*} \times \sqrt{\tilde{\delta}_p \left(\kappa^{L-2} \times \gamma, \xi^{(L)} \right)} \times \left\| \mathcal{N}^{(L-1)}(\mathbf{y}) - \mathcal{N}^{(L-1)}(\mathbf{y}') \right\|_2, \end{aligned}$$

where $\mathbf{y}, \mathbf{y}' \in \mathcal{M}_p^{(L-2)}$ and we have used the fact that $\mathcal{R}^{(L-1)}$ is Lipschitz continuous. Similarly, applying (B.1) and (B.2) recursively to each $\mathcal{N}^{(L-1)}, \dots, \mathcal{N}^{(2)}$ and using the union bound we have $\forall \mathbf{x}, \mathbf{x}' \in \mathcal{M}_p^{(0)} \subset \mathcal{M}^{(0)}$:

$$(B.4) \quad \begin{aligned} \left\| \mathcal{N}(\mathbf{x}) - \mathcal{N}(\mathbf{x}') \right\|_2^2 & \leq c \prod_{i=2}^L \left(\tilde{\delta}_p \left(\kappa^{i-2} \times \gamma, \xi^{(i)} \right) \right)^{\frac{1}{2^{(L-i+1)}}} \|\mathbf{x} - \mathbf{x}'\|_2^2 \\ & \leq c \varepsilon_p \prod_{i=2}^L \left(\tilde{\delta}_p \left(\kappa^{i-2} \times \gamma, \xi^{(i)} \right) \right)^{\frac{1}{2^{(L-i+1)}}} = \delta_p^{\mathcal{N}} \left(\gamma, \xi^{(2)}, \dots, \xi^{(L)} \right), \end{aligned}$$

holds with probability at-least $\left(1 - \sum_{i=2}^L \xi^{(i)} - \sum_{i=2}^L \mathcal{E}_p^{(i)}(m_p, \xi^{(i)}\varepsilon)\right)$, and ε_p is defined as $\varepsilon_p = \sup_{\mathbf{x}, \mathbf{x}' \in \mathcal{M}_p^{(0)}} \|\mathbf{x} - \mathbf{x}'\|_2$. Now in the limit $m_p \rightarrow \infty$, (B.4) holds with probability at-least

$\left(1 - \sum_{i=2}^L \xi^{(i)}\right)$, where the stability function $\tilde{\delta}_p(\gamma, \xi^{(2)})$ (for $i=2$) from (3.11) simplifies as:

$$\tilde{\delta}_p \left(\gamma, \xi^{(2)} \right) = \frac{1}{\xi^{(2)} \times m^2} \sum_{\mathbf{x}_i, \mathbf{x}_j \in C_p} \left\| \mathcal{N}_{\theta^*(\gamma)}^{(2)}(\mathbf{x}_i) - \mathcal{N}_{\theta^*(\gamma)}^{(2)}(\mathbf{x}_j) \right\|_2^2,$$

and the subsequent functions $\tilde{\delta}_p(\kappa^{i-2} \times \gamma, \xi^{(i)})$ for $i > 2$ follows a similar pattern. Further note that from (3.14) we also have $\tilde{\delta}_p(\gamma^u, \xi^{(2)}) = 0$ and $\tilde{\delta}_p(0, \xi^{(2)}) > 0, \forall p$. Therefore, we have $\delta_p^{\mathcal{N}}(\gamma^u, \xi^{(2)}, \dots, \xi^{(L)}) = 0$ and $\delta_p^{\mathcal{N}}(0, \xi^{(2)}, \dots, \xi^{(L)}) > 0, \forall p$, thereby satisfying condition 1 (with $\varepsilon = 0$) for any fixed $\xi^{(2)}, \dots, \xi^{(L)}$. In addition, since each $\tilde{\delta}_p(\kappa^{i-2} \times \gamma, \xi^{(i)})$ is continuous

with respect to γ as proved in [Proposition 3.9](#), $\delta_p^{\mathcal{N}}(\gamma, \xi^{(2)}, \dots, \xi^{(L)})$ is also continuous with respect to γ thereby satisfying condition 2 of [Definition 3.2](#).

Appendix C. Gradients for layerwise training. Consider training the $(i+1)^{th}$ layer. Let us denote the different loss components for a particular j^{th} training sample belonging to cluster C_p as follows:

$$(C.1) \quad \begin{aligned} & \Phi_d(\mathbf{Y}_j^{(o)}), \quad (\text{data loss}) \\ & \Phi_m^{(i+1)}(\mathbf{Y}_j^{(i+1)}) = \frac{\gamma^{(i+1)}}{m_p^2} \times \sum_m \beta_p \left\| \mathbf{Y}_j^{(i+1)} - \mathbf{Y}_m^{(i+1)} \right\|^2 = \gamma^{(i+1)} \times \Phi_m(\mathbf{Y}_j^{(i+1)}), \\ & \Phi_p^{(i+1)}(\mathbf{Y}_j^{(o)}) = \tau^{(i+1)} \times \Phi_p(\mathbf{Y}_j^{(o)}), \quad (\text{physics loss}) \end{aligned}$$

where, $\mathbf{Y}_j^{(i+1)}$ represents the output of the $(i+1)^{th}$ layer for the j^{th} training sample and $\mathbf{Y}_j^{(o)}$ represents the output of the network. Therefore, training problem for the new $(i+1)^{th}$ layer can be formulated as:

$$(C.2) \quad \begin{aligned} & \min_{\mathbf{b}^{(i+1)}, \mathbf{W}^{(i+1)}, \mathbf{W}_{\text{pred}}, \mathbf{b}_{\text{pred}}} \Phi_d(\mathbf{Y}_j^{(o)}) + \Phi_m^{(i+1)}(\mathbf{Y}_j^{(i+1)}) + \Phi_p^{(i+1)}(\mathbf{Y}_j^{(o)}) \\ & \text{such that:} \\ & \mathbf{Y}_j^{(i+1)} = \mathcal{R}^{(i)}(\mathbf{Y}_j^{(i)}) + h^{(i+1)}(\mathbf{W}^{(i+1)} \mathcal{R}^{(i)}(\mathbf{Y}_j^{(i)}) + \mathbf{b}^{(i+1)}), \\ & \mathbf{Y}_j^{(o)} = h_{\text{pred}}(\mathbf{W}_{\text{pred}} \mathcal{R}^{(i+1)}(\mathbf{Y}_j^{(i+1)}) + \mathbf{b}_{\text{pred}}). \end{aligned}$$

The Lagrangian for the above constrained optimization problem is defined as:

$$(C.3) \quad \begin{aligned} \mathcal{L}_j = & \Phi_d(\mathbf{Y}_j^{(o)}) + \Phi_m^{(i+1)}(\mathbf{Y}_j^{(i+1)}) + \Phi_p^{(i+1)}(\mathbf{Y}_j^{(o)}) \\ & + (\lambda_2)^T \left[\mathbf{Y}_j^{(o)} - h_{\text{pred}}(\mathbf{W}_{\text{pred}} \mathcal{R}^{(i+1)}(\mathbf{Y}_j^{(i+1)}) + \mathbf{b}_{\text{pred}}) \right] \\ & + (\lambda_1)^T \left[\mathbf{Y}_j^{(i+1)} - \mathcal{R}^{(i)}(\mathbf{Y}_j^{(i)}) - h^{(i+1)}(\mathbf{W}^{(i+1)} \mathcal{R}^{(i)}(\mathbf{Y}_j^{(i)}) + \mathbf{b}^{(i+1)}) \right]. \end{aligned}$$

The first order optimality conditions are as follows:

$$(C.4) \quad \frac{\partial \mathcal{L}_j}{\partial \mathbf{Y}_j^{(i+1)}} = 0, \quad \frac{\partial \mathcal{L}_j}{\partial \mathbf{Y}_j^{(o)}} = 0, \quad \frac{\partial \mathcal{L}_j}{\partial \mathbf{W}^{(i+1)}} = 0, \quad \frac{\partial \mathcal{L}_j}{\partial \mathbf{b}^{(i+1)}} = 0, \quad \frac{\partial \mathcal{L}_j}{\partial \mathbf{W}_{\text{pred}}} = 0, \quad \frac{\partial \mathcal{L}_j}{\partial \mathbf{b}_{\text{pred}}} = 0.$$

$$\frac{\partial \mathcal{L}_j}{\partial \mathbf{Y}_j^{(i+1)}} = 0 \implies \lambda_1 = \mathbf{R}^{(i+1)} \mathbf{W}_{\text{pred}}^T \left[h'_{\text{pred}}(\mathbf{W}_{\text{pred}} \mathcal{R}^{(i+1)}(\mathbf{Y}_j^{(i+1)}) + \mathbf{b}_{\text{pred}}) \circ \lambda_2 \right] - \frac{\partial \Phi_m^{(i+1)}}{\partial \mathbf{Y}_j^{(i+1)}},$$

where $\mathcal{R}^{(i+1)}(\mathbf{Y}_j^{(i+1)}) = \mathbf{R}^{(i+1)} \mathbf{Y}_j^{(i+1)} + \mathbf{b}_r$ such that $\mathbf{R}^{(i+1)}$ is a diagonal matrix and \mathbf{b}_r is a constant vector. Similarly, other optimality conditions can be derived as follows:

$$\frac{\partial \mathcal{L}_j}{\partial \mathbf{Y}_j^{(o)}} = 0 \implies \lambda_2 = - \left(\frac{\partial \Phi_d}{\partial \mathbf{Y}_j^{(o)}} + \frac{\partial \Phi_p^{(i+1)}}{\partial \mathbf{Y}_j^{(o)}} \right),$$

$$(C.5) \quad \frac{\partial \mathcal{L}_j}{\partial \mathbf{W}^{(i+1)}} = - \left[\lambda_1 \circ \left(h^{(i+1)} \right)' \left(\mathbf{W}^{(i+1)} \mathcal{R}^{(i)} \left(\mathbf{Y}_j^{(i)} \right) + \mathbf{b}^{(i+1)} \right) \right] \left(\mathcal{R}^{(i)} \left(\mathbf{Y}_j^{(i)} \right) \right)^T,$$

$$(C.6) \quad \frac{\partial \mathcal{L}_j}{\partial \mathbf{b}^{(i+1)}} = - \lambda_1 \circ \left(h^{(i+1)} \right)' \left(\mathbf{W}^{(i+1)} \mathcal{R}^{(i)} \left(\mathbf{Y}_j^{(i)} \right) + \mathbf{b}^{(i+1)} \right),$$

$$(C.7) \quad \frac{\partial \mathcal{L}_j}{\partial \mathbf{W}_{\text{pred}}} = - \left[\lambda_2 \circ h'_{\text{pred}} \left(\mathbf{W}_{\text{pred}} \mathcal{R}^{(i+1)} \left(\mathbf{Y}_j^{(i+1)} \right) + \mathbf{b}_{\text{pred}} \right) \right] \left(\mathcal{R}^{(i+1)} \left(\mathbf{Y}_j^{(i+1)} \right) \right)^T,$$

$$(C.8) \quad \frac{\partial \mathcal{L}_j}{\partial \mathbf{b}_{\text{pred}}} = - \left[\lambda_2 \circ \left(h'_{\text{pred}} \left(\mathbf{W}_{\text{pred}} \mathcal{R}^{(i+1)} \left(\mathbf{Y}_j^{(i+1)} \right) + \mathbf{b}_{\text{pred}} \right) \right) \right].$$

Appendix D. Proof of Proposition 3.20 .

Proof. First note that \mathcal{Q}_i is Lipschitz continuous when employing Lipschitz continuous activation functions. Therefore, we have $\forall \mathbf{x}, \mathbf{x}' \in \mathcal{M}_p^{(0)}$:

$$(D.1) \quad \begin{aligned} \|\mathcal{Q}(\mathbf{x}) - \mathcal{Q}(\mathbf{x}')\|_2 &= \|\mathcal{Q}_2(\mathbf{x}) + \dots \mathcal{Q}_{r-1}(\mathbf{x}) - (\mathcal{Q}_2(\mathbf{x}') + \dots \mathcal{Q}_{r-1}(\mathbf{x}')\|_2 \\ &\leq \|\mathcal{Q}_2(\mathbf{x}) - \mathcal{Q}_2(\mathbf{x}')\|_2 + \dots \|\mathcal{Q}_{r-1}(\mathbf{x}) - \mathcal{Q}_{r-1}(\mathbf{x}')\|_2 \\ &\leq \mathcal{L}^{(2)} \left(\mathcal{M}_p^{(0)} \right) \times \varepsilon_p + \dots \mathcal{L}^{(r-1)} \left(\mathcal{M}_p^{(0)} \right) \times \varepsilon_p, \end{aligned}$$

where $\mathcal{L}^{(i)}(\mathcal{M}_p^{(0)})$ is the local Lipschitz constant of \mathcal{Q}_i with respect to $\mathcal{M}_p^{(0)}$, and $\varepsilon_p = \sup_{\mathbf{x}, \mathbf{x}' \in \mathcal{M}_p^{(0)}} \|\mathbf{x} - \mathbf{x}'\|_2$. Now note that $\mathcal{L}^{(i)}(\mathcal{M}_p^{(0)}) \leq \mathcal{L}^{(i)}(\mathbb{R}^S)$ since $\mathcal{M}_p^{(0)} \subset \mathcal{M}^{(0)} \subset \mathbb{R}^S$. Further, noting the fact that the network \mathcal{Q}_i is a composition of Lipschitz functions, we have for each i :

$$(D.2) \quad \begin{aligned} \mathcal{L}^{(i)}(\mathcal{M}_p^{(0)}) \times \varepsilon_p &\leq \mathcal{L}^{(i)}(\mathbb{R}^S) \times \varepsilon_p \leq \left(\prod_{k=1}^3 \|\mathbf{w}_i^{(k)}\|_2 \right) \times \varepsilon_p \\ &\leq \ell^3 \times \left[\prod_{k=1}^3 \left(\sum_{l=0}^m \left\| \left(\mathbf{g}_l^{(k)} \right)_i \right\|_2 \right) \right] \times \varepsilon_p \end{aligned}$$

where the last line follows from the standard gradient descent update formulae and applying a triangle inequality, $\left(\mathbf{g}_l^{(k)} \right)_i$ represents the gradients for the k^{th} layer weight matrix at the l^{th} iteration of gradient descent algorithm for network \mathcal{Q}_i . Applying the transformation $\zeta = \frac{1}{m+1}$, and combining (D.1) and (D.2) we can recover the stability function that satisfies condition 3 as follows:

$$\|\mathcal{Q}(\mathbf{x}) - \mathcal{Q}(\mathbf{x}')\|_2 \leq \sum_{i=2}^{r-1} \ell^3 \times \left[\prod_{k=1}^3 \left(\sum_{l=0}^{(1/\zeta)-1} \left\| \left(\mathbf{g}_l^{(k)} \right)_i \right\|_2 \right) \right] \times \varepsilon_p = \sum_{i=2}^{r-1} \delta_p^{(i)}(\zeta) = \delta_p^{\mathcal{Q}}(\zeta).$$

Now in order to ensure that $\delta_j^Q(\zeta)$ is a valid stability function as per [Definition 3.4](#), it is enough to check if each $\delta_p^{(i)}(\zeta)$ satisfies condition 1 in [Definition 3.2](#), and condition 3 in [Definition 3.4](#).

Note that $\delta_j^{(i)}(\zeta)$ is now a discrete function with domain $\left\{\frac{1}{m^{u+1}}, \frac{1}{m^u}, \dots, 1\right\}$, where $m^u \in \mathbb{Z}^+$ is some chosen upper bound for the training iterations. Note that $\delta_p^{(i)}(1) = 0$ since $\left(\mathbf{g}_0^{(3)}\right)_i = \mathbf{0}$ due to the output layer being initialized with zeros in [Algorithm 2.2](#). Further, $\delta_p^{(i)}\left(\frac{1}{m^{u+1}}\right) > 0$ since the gradients in the subsequent iterations must be non-zero for decreasing the loss. Therefore, we have $\delta_p^{(i)}(1) < \delta_p^{(i)}\left(\frac{1}{m^{u+1}}\right)$ satisfying condition 1 in [Definition 3.2](#). In addition, it is clear that $\delta_p^{(i)}(\zeta)$ is monotonically decreasing with respect to ζ thereby satisfying condition 3 in [Definition 3.4](#).

Appendix E. General setting for numerical experiments. All codes were written in Python using TensorFlow. Throughout the study, we have employed the Adam optimizer [25] for minimizing the cost function. The manifold regularization term is computed over mini-batches. We consider a decay of manifold regularization weight $\gamma^{(i+1)} = 0.5 \times \gamma^{(i)}$ on adding a new layer unless otherwise stated. We choose $\beta_p = 1, \forall p$ in (2.3). Our proposed approach is compared with a number of different approaches. Description of different algorithms adopted for comparison with the proposed approach

Algo. 2.1 : layerwise training algorithm described in [subsection 2.1](#).

Algo. 2.2 : Sequential residual learning after Algo. 2.1 ([subsection 2.2](#)).

Baseline network : A fully-connected deep neural network with the same depth and width as that produced by [Algorithm 2.1](#).

Algo. 2.2 (1 network) : Sequential residual learning after Algo. 2.1 using 1 network in [Algo. 2.2](#) trained for a large number of epochs.

Baseline + Algo. 2.2 : [Algorithm 2.2](#) applied on top of the residuals produced by the baseline network.

Forward Thinking : Algorithm for layerwise adaptation by Hettinger et al. [22]. This strategy is also similar to the algorithm by Belilovsky et al. [2] and Trinh et al. [51].

Approach [22]+ Algo. 2.2 : [Algorithm 2.2](#) applied on top of the residuals produced by Forward thinking [22].

Architecture Search (AS) : Random search with early stopping proposed by Liam Li and Ameet Talwalkar [30].

When training the baseline, 100 different random initializations are considered and the best result is chosen for comparison. For architecture search (AS), the search space is defined by setting the maximum width (for each hidden layer) and maximum depth the same as that produced by [Algorithm 2.1](#).

E.1. Choice of $\mathcal{R}^{(i)}$. For the results provided in this work, we choose $\mathcal{R}^{(i)}$ in (2.1) as

the identity map for computational efficiency. This avoids recomputing the map $\mathcal{R}^{(i)}$ in each training iteration. We observed numerically that the feature scaling introduced in (2) from a pure theoretical purpose did not provide improvement in results.

E.2. Tuning parameters γ and ζ for δ -stability. Note that the hyperparameters γ (in Algorithm 2.1) and E_e (in Algorithm 2.2) are tuned based on the validation dataset to achieve the best results. The best parameters are the ones that minimize the validation loss such as depicted in Figure 2. Note that tuning parameter E_e in Algorithm 2.2 corresponds to tuning the parameter ζ in proposition 3.20. We consider a strategy of training the first two networks in Algorithm 2.2 for E_e^1 number of epochs and training the remaining networks for E_e^2 number of epochs. This leads to tuning $\{E_e^1, E_e^2\}$ in Algorithm 2.2. That is, Algorithm 2.2 is run for different choices of $\{E_e^1, E_e^2\}$ and the best choice is the one that provides the lowest validation loss. This strategy is adopted since the residuals become increasingly nonlinear and subsequent networks require more number of epochs to promote training (i.e. decrease the loss).

Appendix F. Boston house price prediction problem. For this problem, the manifold regularization is computed by employing the K-means clustering algorithm on the input features [35] and the number of clusters K is chosen as 5.

Appendix G. Physics informed adaptive neural network (PIANN). This section contains additional details on the PIANN problem discussed in subsection 4.2. The relative L^2 error achieved after adding each layer is shown in Table 2 (case a) and Table 5 (case b). The active parameters in each hidden layer is shown in Table 3 (case a) and Table 6 (case b). The results achieved by the baseline network as well as other layerwise training method [22] is also provided in Table 4 (case a) and Table 7 (case b).

Table 2

Relative L^2 error on layer addition (Case a)

Layer No.	$\tau^{(i)}$	Relative L^2 error
2	10	1.723×10^{-1}
3	15	2.254×10^{-2}
4	20	4.974×10^{-3}
5	25	6.649×10^{-4}
6	30	2.660×10^{-4}
7	35	6.720×10^{-5}

Table 3

% of non-zero parameters in each layer (Case a)

Layer No.	% of non-zero parameters
2	99.5 %
3	97.7 %
4	98.9 %
5	95.4 %
6	92.5 %
7	96.7 %

Appendix H. Interpretability of hidden layers and transfer learning strategy. In this section, we demonstrate how the interpretability of different layers in PIANN helps one in devising efficient transfer learning strategies and make informed decisions on which layers to re-train. For demonstration, consider the operator in (4.5) with $a(x_1, x_2) = e^{x_1+x_2}$ and $f = 200$. We reuse the pre-trained model that learnt the solution in Figure 5. The objective is to correct this pre-trained model for the new coefficient $a(x_1, x_2) = e^{x_1+x_2}$.

Table 4*Performance of Baseline Network and other layerwise training methods (Case a)*

Method	Relative L^2 error	Parameters trained simultaneously
Proposed method	6.7×10^{-5}	10,501
Baseline network	1.0×10^{-4}	61,001
Forward Thinking [22]	9.2×10^{-2}	10,501

Table 5*Relative L^2 error on layer addition (Case b)*

Layer No.	$\tau^{(i)}$	Relative L^2 error
2	5	3.59×10^{-1}
3	10	4.75×10^{-2}
4	15	1.13×10^{-3}
5	20	7.86×10^{-5}

Table 6*% of non-zero parameters in each layer (Case b)*

Layer No.	% of non-zero parameters
2	97.52 %
3	91.29 %
4	97.35 %
5	90.00%

Table 7*Performance of Baseline Network and other layerwise training methods (Case b)*

Method	Relative L^2 error	Parameters trained simultaneously
Proposed method	7.8×10^{-5}	10,501
Baseline network	1.1×10^{-4}	40,801
Forward Thinking [22]	1.6×10^{-2}	10,501

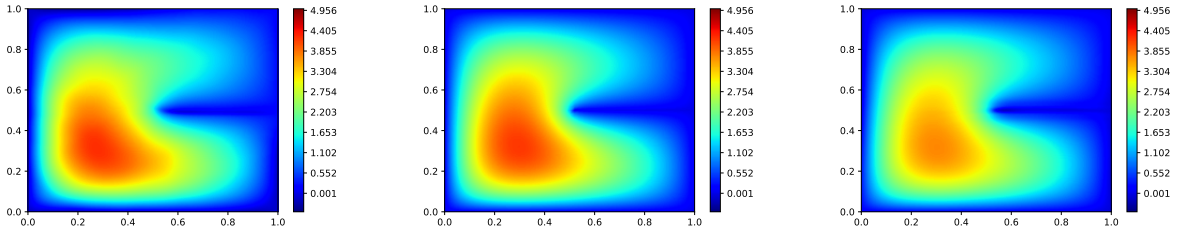


Figure 12. Transfer learning strategy. Left to right: Transfer learning on interpretable network achieved by our approach (relative L^2 error= 4.432×10^{-3} at the end of 100 epochs); True solution; Traditional transfer learning strategy on a baseline (relative L^2 error= 8.72×10^{-3} at the end of 100 epochs).

Since in our approach (PIANN), the first few layers focus mainly on enforcing the boundary conditions (Figure 5) it is anticipated that only the last layers needs retraining for model correction. In our approach for transfer learning, we consider retraining the last two layers reinitialized with zero weights and biases. The relative L^2 error achieved and the learnt solution after retraining the last two layers for 100 epochs is shown in Figure 12. In addition,

we also consider the traditional transfer learning strategy of retraining the last two layers of a pre-trained baseline network that lacks the interpretability of its layers [49]. Note that in this case it is unclear on the best layers to re-train and a discussion on this aspect is provided in [49]. Comparison of efficiency between the two approaches is shown in Figure 12. It is clear from Figure 12 that our approach learns the new solution faster in comparison to the traditional transfer learning approach.

Appendix I. Performance on MNIST dataset.

I.1. Training with 20 neurons in each hidden layer. The inputs for this experiment is given in Appendix J. The parameter efficiency achieved for the case of using 20 neurons in the hidden layers is provided in Figure 13. Table 8 shows the comparison of results with baseline and other layerwise training method.

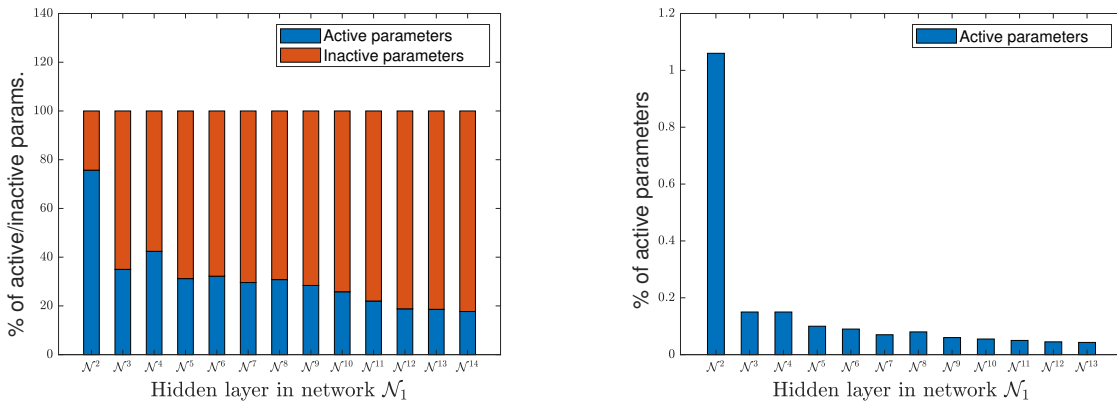


Figure 13. Left to right: Active and inactive parameters in each hidden layer (20 neurons in each hidden layer); Active and inactive parameters in each hidden layer (500 neurons in each hidden layer)

Table 8

MNIST: Performance of baseline network and other layerwise training methods (20 neuron case)

Method	Test Accuracy %	Parameters trained simultaneously
Proposed method	96.90	16,330
Baseline network	96.00	21,370
Baseline + Algo. 2.2	95.90	21,370
Forward Thinking [22]	95.90	16,330
Approach [22] + Algo. 2.2	96.00	16,330
Architecture search (AS)	96.47	-

Note that our experiments showed that, forward thinking model [22] quickly over-fits on the training data while adding the initial few layers. Further, forward thinking model is not δ -stable which is a necessary condition for Algorithm 2.2 to achieve robustness (Remark 3.21).

Numerically, it is observed that the residual defined in line 4 of [Algorithm 2.2](#) is very low in magnitude, and it is hardly possible to extract information from the residual and improve the results. Hence, the performance of forward thinking model + [Algorithm 2.2](#) has been not included in the comparison results shown in [Figure 10](#) since the behaviour is similar to baseline+[Algorithm 2.2](#).

I.2. Training with 500 neurons in each hidden layer. The parameter efficiency and the comparison of results with baseline is shown in [Figure 13](#) and [Table 9](#).

Table 9

MNIST: Performance of baseline network and other layerwise training methods (500 neuron case).

Method	Test accuracy %	Params. trained simultaneously
Proposed method	98.7	6,48010
Baseline network	98.2	34,03510
Baseline + Algo. 2.2	98.2	34,03510
Forward Thinking [22]	98.3	6,48010
Approach [22] + Algo. 2.2	98.4	6,48010
Architecture search (AS)	98.3	-

Appendix J. Details of input parameter values for different problems. The description of each problem is given below:

- I : Boston house price prediction problem
- II (a) : Physics informed adaptive neural network (PIANN), Symmetric boundary.
- II (b) : Physics informed adaptive neural network (PIANN), Slit in the Domain.
- III (a) : Adaptive learning for inverse problems (20 data-set problem).
- III (b) : Adaptive learning for inverse problems (50 data-set problem).
- IV (a) : MNIST classification (20 neuron in hidden layers).
- IV (b) : MNIST classification (500 neuron in hidden layers).

Details of input parameters used in [Algorithm 2.1](#) is provided in [Table 10](#). ℓ represents the learning rate, d_l represent the decay of learning rate, and E_e represents the number of epochs for which each layer is trained. Details of input parameters used in [Algorithm 2.2](#) is provided in [Table 11](#). In [Table 11](#), Epoch $\{E_e^1, E_e^2\}$ means that the first two networks in [Algorithm 2.2](#) is trained for E_e^1 number of epochs and the remaining networks are trained for E_e^2 number of epochs.

⁶FC represents fully connected network.

Table 10*Details of input parameters in Algorithm 2.1 for different problems*

Problem	ε_η	ρ	$(\alpha^{(2)}, \tau^{(2)}, \gamma^{(2)})$	ℓ	d_l	E_e	N_o	Batch size
I	0.035	10^{-6}	(0.05, 0, 0.06)	0.001	0.9	50	100	70
II (a)	0.8	10^{-6}	(0.001, 10, 0)	0.0005	1	1000	100	500
II (b)	0.5	10^{-6}	(0.001, 5, 0)	0.0005	1	2000	100	500
III (a)	0.035	10^{-6}	(0.0001, 0, 0.001)	0.001	1	400	100	20
III (b)	0.0015	10^{-6}	(0.0001, 0, 0.001)	0.001	1	400	100	50
IV (a)	0.005	10^{-6}	(0.001, 0, 0.0035)	0.001	0.9	100	20	900
IV (b)	0.005	10^{-6}	(0.001, 0, 0.005)	0.001	0.9	100	500	900

Table 11*Details of input parameters in Algorithm 2.2 for different problems*

Problem	N_n	Network ⁶	Activation	No. of layers	No. of neurons	Epoch E_e $\{E_e^1, E_e^2\}$	Batch size
I	5	<i>FC</i>	<i>relu</i>	1	10	{70, 100}	70
IV (a)	20	<i>FC</i>	<i>elu</i>	2	20	{100, 200}	900
IV (b)	4	<i>FC</i>	<i>elu</i>	2	500	{200, 400}	900